2018

The Influence of Northern Hemisphere Teleconnections on the Geography of Pacific Tropical Cyclone Genesis

Nicholas Ray Adkins
nickadkn@gmail.com

Follow this and additional works at: https://mds.marshall.edu/etd

 Part of the Meteorology Commons, and the Physical and Environmental Geography Commons

THE INFLUENCE OF NORTHERN HEMISPHERE TELECONNECTIONS ON THE GEOGRAPHY OF PACIFIC TROPICAL CYCLONE GENESIS

A thesis submitted to
the Graduate College of
Marshall University
In partial fulfillment of
the requirements for the degree of
Master of Science
In
Geography
by
Nicholas Ray Adkins
Approved by
Dr. Kevin Law, Committee Chairperson
Dr. Jamie Leonard
Dr. Anita Walz

Marshall University
May 2018

APPROVAL OF THESIS

We, the faculty supervising the work of Nicholas Ray Adkins, affirm that the thesis, *The Influence of Northern Hemisphere Teleconnections on the Geography of Pacific Tropical Cyclone Genesis*, meets the high academic standards for original scholarship and creative work established by the Master of Science in Geography Program and the College of Liberal Arts. This work also conforms to the editorial standards of our discipline and the Graduate College of Marshall University. With our signatures, we approve the manuscript for publication.

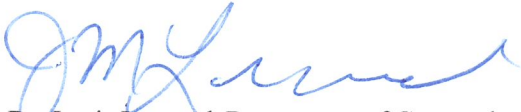|		
Dr. Kevin Law, Department of Geography	Committee Chairperson	4/18/18 — Date
Dr. Jamie Leonard, Department of Geography	Committee Member	4/18/18 — Date
Dr. Anita Walz, Department of Geography	Committee Member	4-18-18 — Date

ACKNOWLEDGEMENTS

The author wishes to express his appreciation to Dr. Kevin Law for the unwavering support throughout the life of this project. Dr. Law was an upstanding advisor with whom the author closely coordinated the structure and methodology of this research. Without his guidance and knowledge, this project would likely have not come to fruition. The author would also like to thank Dr. Jamie Leonard and Dr. Anita Walz for agreeing to be panel members for the defense of this thesis research.

TABLE OF CONTENTS

LIST OF TABLES

LIST OF FIGURES

ABSTRACT

The research in this thesis used statistical and spatial analysis methods to test the influence of six Northern Hemisphere teleconnection patterns on the latitude and longitude components of tropical cyclogenesis occurring in the eastern and western North Pacific Ocean basins for the period 1979-2016. The Pacific-North American (PNA), West Pacific (WP), El Niño Southern Oscillation (ENSO), Pacific Decadal Oscillation (PDO), Madden-Julian Oscillation (MJO), and Quasi-Biennial Oscillation (QBO) teleconnection patterns were examined independently and in combination for association with variations in cyclogenesis geography. Four of the six teleconnection patterns were found to exert an influence on cyclogenesis latitude and/or longitude in their respective areas of dominance during independent testing; the PNA and WP patterns were not found to be significant explanatory variables for cyclogenesis latitude or longitude. Overall, the teleconnection patterns explained a greater portion of the variance in cyclogenesis latitude than longitude for both the eastern and western North Pacific basins. Patterns of cyclogenesis cluster shifting in positive, neutral, and negative phases of each teleconnection were identified for the study area using kernel density analysis. Furthermore, the teleconnection combination analysis was used to test the influence of multiple teleconnection patterns on the geography of tropical cyclones in positive and negative phases. Although the analysis provided statistically significant results, the combination analysis was inefficient at explaining variance in cyclogenesis geography.

CHAPTER 1
INTRODUCTION

The immense size and power of the Pacific Ocean basin is a scientific marvel. With a surface area of over 60 million square miles, the body of water encompasses roughly one third of the earth's surface and easily trumps the planet's total land surface area. Like all large bodies of water, the Pacific Ocean influences climatological and day-to-day weather patterns across a vast area of land and sea. In combination with global wind flows and large-scale ocean currents, the Pacific Ocean plays a dynamic role in the distribution of the sun's energy across the globe. Areas of low latitude, also known as the "tropics," receive the most radiation from the sun as incoming rays penetrate the atmosphere at the most direct angle. As large pools of water like the Pacific Ocean are heated by incoming solar radiation, the amount of water vapor in the air (humidity) increases and rain clouds often form as the warm air naturally rises into the troposphere and condenses as it cools with height. The rising air often creates turbulent storm clouds and storm systems that, at peak saturation, produce precipitation that falls back to earth as rain or snow and the water cycle repeats (Rohli and Vega 2012).

In very unstable atmospheric conditions over large bodies of warm water, the aforementioned low-level disturbances can continue to grow and develop into tropical cyclones. The term "tropical cyclone" is a blanket term that is used to describe organized, rotating thunderstorm activity over tropical or subtropical waters. In the Atlantic and eastern North Pacific Ocean basins, these storm systems are known as "hurricanes." Likewise, they are known as "typhoons" in the western North Pacific basin and simply "cyclones" in the Southwest Pacific basin and Indian Ocean (Rohli and Vega 2012). For the purposes of this study, the term tropical cyclone will be used regardless of in which basin the storm occurs.

The life cycle of an intense low-pressure system goes through multiple stages of development before it can be classified as a tropical cyclone. Most storms begin as a tropical disturbance; a small cluster of thunderstorm clouds that have very weak rotation and convection that often seem like a normal, non-threatening, thunderstorm. With the right atmospheric conditions, however, the storm will continue to strengthen, gaining rotational speed and convection as hot air is forced upwards into the troposphere and the billowing storm clouds continue to grow. If sustained wind speeds increase to 20 knots upwards to 34 knots (23-38 mph), the storm status is upgraded to a tropical depression as the atmospheric pressure at the center of the storm continues to drop. At 35 knots (39 mph), the depression is upgraded to a tropical storm and has well defined characteristics like a calm central core called an eye, a turbulent eye wall, and rain bands circulating around the central eye of the storm. At this point, the storm also receives a name from a pre-defined list for each ocean basin from the World Meteorological Organization. Under the most favorable conditions, the storm will continue to strengthen and develop into a tropical cyclone whenever sustained wind speeds reach 64 knots (74 mph) (NOAA Hurricane Research Division n.d.).

The Pacific Ocean basin is the most active in the world for tropical cyclone activity. More specifically, the western North Pacific basin is the most producing region for tropical cyclones on earth. According to the National Oceanic and Atmospheric Administration (NOAA) Hurricane Research Division, the western North Pacific basin averaged 26 storms per year with wind speeds greater than 39 mph from 1981-2016. Furthermore, the region averaged 16.5 tropical cyclones with wind speeds greater than 74 mph. The eastern North Pacific basin was the second most active with an average of 16.6 named storms and 8.9 tropical cyclones for the same period (NOAA Hurricane Research Division n.d.).

The very complex nature of tropical cyclone formation has been under study for quite some time, with particular attention being focused on the "why" and "where" factors associated with their development. A multitude of environmental factors have an influence on tropical cyclone genesis. Major storm systems need the perfect combination of warm sea surface temperatures (SSTs), upper level wind divergence, low-level convection, low wind shear, and Coriolis force to produce the "perfect storm." The absence of just one of the aforementioned parameters can disrupt tropical cyclone growth and keep the storm from becoming a powerful force of nature.

The most vital ingredient that is needed for tropical cyclone development is a large pool of warm water with a sea surface temperature (SST) above 26° to 27°C (79°-80°F); (Palmén 1956; Ramage 1959; Gray 1975; Whitney and Hobgood 1997). At this temperature, the atmosphere above the warm ocean water becomes very unstable and makes severe thunderstorm activity much more likely. An atmospheric disturbance and low-level convection provide the right recipe for a low-pressure system to develop. If the pressure gradient continues to intensify, deep convection occurs and tropical cyclones begin to develop. As the warm air rises, it condenses in the cooler air aloft and releases latent heat that drives the tropical cyclone circulation (Ramage 1959; Emanuel 1987). It has also been proven that for major tropical cyclones to develop, a deep pool of warm water (roughly 150 feet) is needed in order to sustain the convective energy of the tropical cyclone (Gray 1979).

Weak vertical wind shear and the Coriolis effect allow tropical cyclones to begin rotation and build vertically in the atmosphere as convection and condensation increase over the warm central core and cumulonimbus clouds rise into the upper troposphere. Wind shear occurs whenever wind direction changes throughout the vertical component of the atmosphere and is

detrimental to tropical cyclones because it alters the heat exchange process that drives their development (Palmén 1956; Ramage 1959). The Coriolis force is a result of the area around the equator rotating faster on earth's axis than that of the area around the poles. The circumference of earth is much larger at the equator than at the poles, therefore it must spin faster on its axis at low latitudes to complete the same 24-hour daily rotation that occurs at the poles with a much smaller circumference. As a result, any fluid motion occurring between the equator and the poles is subject to the "Coriolis Effect" as it travels across or above the Earth's surface. In the Northern Hemisphere, the Coriolis Effect causes an apparent deflection to the right as the object moves over the spherical surface of the earth. For tropical cyclones, the Coriolis force creates the counter-clockwise rotation that all low-pressure storms inherit in the Northern Hemisphere. As the low-pressure center of the tropical cyclone attracts air from regions of higher pressure, it is bent to the east (right) by the deflection of the Coriolis effect. At the equator, Coriolis force is not present and therefore tropical cyclones do not form there (Rohli and Vega 2012).

Another key influence on tropical cyclone development are large-scale atmospheric circulation patterns called teleconnections. John M. Wallace and David S. Gutzler (1981) best describe teleconnections as "significant simultaneous correlations between temporal fluctuations in meteorological parameters at widely separated points on earth." The meteorological parameters mentioned by Wallace and Gutzler generally refer to fluctuations in either SST, sea level pressure (SLP), or geopotential height in the atmosphere. The authors go on to explain some of the methodology that scientists have used in the past to define teleconnection indices:

> For example, some investigators have used time series of sea level pressure at some particular station as a basis for correlating or compositing atmospheric data in order to define the teleconnection patterns; some have used time series of sea

level pressure differences between selected pairs of stations; some have used time

series consisting of linear combinations of sea-level pressure at three or more

stations; others have used time series based on parameters such as surface

temperature or upper level geopotential height, or combinations of different

parameters (Wallace and Gutzler 1981).

Since total atmospheric mass is always conserved, teleconnections act in "see-saw"

patterns. For example, as the SLP increases in one region, it must decrease in another. Because

of this reason, teleconnections are generally classified in positive, neutral (normal), and negative

phases.

Teleconnections have a considerable influence on climatic variability and overall weather

phenomena in their respective areas of dominance (Shimura, Mori, and Mase 2013). The

atmospheric patterns control global wind flows that have drastic climatic implications, influence

large-scale weather events like tropical cyclones, and even control markets and economies of

regions that they impact. In the Northern Hemisphere alone there are more than ten

teleconnection patterns that exert an influence on weather and climate (Wallace and Gutzler

1981; Rohli and Vega 2012).

The research in this thesis focuses on Pacific tropical cyclone geography and the

influence of Northern Hemisphere teleconnection patterns. It has been proven (Angell,

Korshover, and Cotten 1969; Klotzbach and Gray 2004; Linkin and Nigam 2008; Choi and

Moon 2012) that teleconnection fluctuations have an influence on tropical cyclone activity across

multiple ocean basins; however, very little research has been published on the influence that

teleconnections have on the geography of tropical cyclone formation. The objective of this thesis

is to test the correlation between variations in tropical cyclone geography with the fluctuation of

teleconnection patterns. Statistical and spatial analysis methods will be used to uncover correlations between teleconnection patterns and alterations in Pacific tropical cyclone geography. The research examines 37 years of tropical cyclone activity from 1979-2016 in both the eastern and western North Pacific Ocean basins totaling nearly 1,600 tropical cyclones. In Chapter 2, each teleconnection pattern used in this study is examined in further detail before presenting the Methodology and Results in Chapters 3 and 4, respectively. Chapters 5 and 6 provide further discussion and the thesis conclusion.

CHAPTER 2
REVIEW OF THE LITERATURE

Multiple teleconnection patterns were used in this study in order to test numerous atmospheric parameters against the geography of tropical cyclogenesis. Each teleconnection has defining characteristics such as their geographic influence, length of progression and phases, and overall volatility. Six teleconnection patterns measured by seven indices were used in this research; the Pacific-North American (PNA) teleconnection, the Western Pacific (WP) teleconnection, the El Niño Southern Oscillation (ENSO); (measured by the Southern Oscillation Index (SOI), and Multivariate El Niño Southern Oscillation Index (MEI)), the Madden-Julian Oscillation (MJO), the Pacific Decadal Oscillation (PDO), and the Quasi-Biennial Oscillation (QBO). In the following sub-sections, each teleconnection pattern will be explained in order to get a firm understanding of the characteristics and typical effects that the teleconnection exerts on the area of influence.

Pacific-North American (PNA)

One of the largest influences of weather and climatic patterns in North America is the PNA teleconnection. Since the PNA has the greatest influence on the mid-Pacific and locations to the east, the PNA was only tested in the eastern North Pacific basin. The PNA is a representation of the fluctuation in mid-tropospheric geopotential height, or height of a certain pressure level in our atmosphere, over the mid-Pacific and eastward spanning the North American continent (Stoner, Hayhoe, and Wuebbles 2009; Rohli and Vega 2012). According to Wallace and Gutzler (1981), the PNA index is defined as a combination of normalized 500 millibar (mb) geopotential height anomalies at four pattern centers in the North Pacific and over North America. The first measurement center is located near Hawaii (20°N, 160°W), with a

second over the North Pacific Ocean near the Aleutian Low (45°N, 165°W). The third

measurement location is over Alberta, Canada (55°N, 115°W), and the fourth is over the Gulf

Coast of the United States (30°N, 85°W; Wallace and Gutzler 1981).

The positive (negative) phase of the PNA is present whenever geopotential heights are

above average (below average) near Hawaii and Alberta, and below average (above average)

over the Aleutian Low and the Gulf Coast (Figure 2.1; Stoner et al. 2009). An eastward shift in

the exit region of the East Asian jet stream near the western U.S. coast influences the positive

phase of PNA with increased geopotential heights in western Canada and Hawaii (Stoner et al.

2009). In the negative phase, the jet stream retracts back toward East Asia and splits the jet

stream with below average geopotential heights over western Canada and Hawaii (Wallace and

Gutzler 1981).
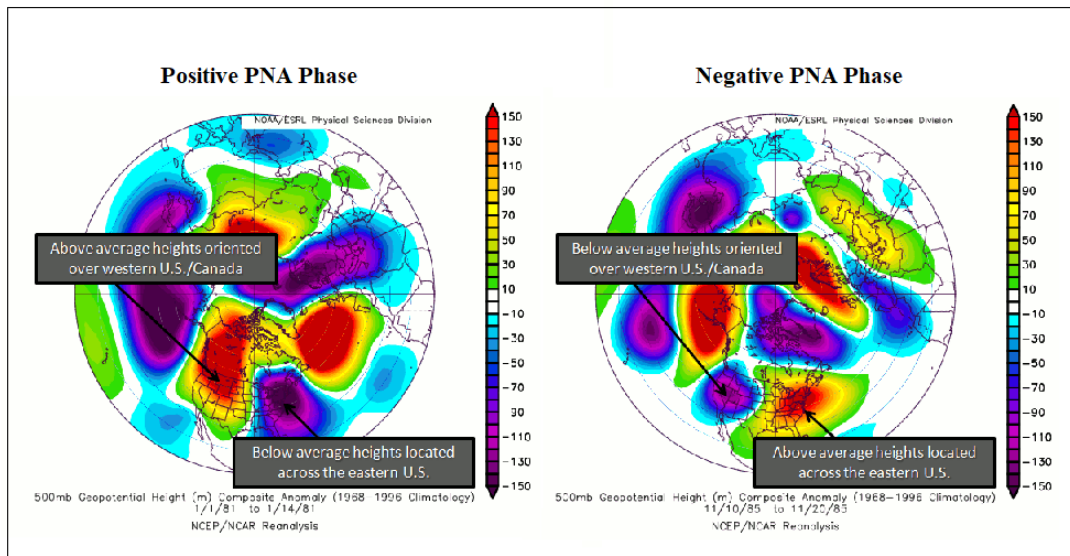
Figure 2.1. Sample flow of the PNA teleconnection in the positive and negative phase.
(Data: https://climate.ncsu.edu/climate/patterns/pna)

Although the PNA has been correlated with fluctuations in tropical cyclone activity over the Atlantic basin (Klotzbach and Gray 2004), the teleconnection is not widely known to have dramatic impacts on tropical cyclones in the North Pacific Basin. However, the teleconnection is closely influenced by ENSO and could mimic similar influences on tropical cyclogenesis in the eastern North Pacific basin. Since the PNA is a measure of geopotential height anomalies and overall mid-tropospheric flow, the teleconnection pattern could also have an influence on cyclogenesis location or tropical cyclone track after the initial formation.

West Pacific (WP)

Like the PNA pattern discussed in the previous section, the WP teleconnection is a measurement of the variability in 500 mb geopotential height between set action centers. Since the teleconnection is measured over the western North Pacific basin, the WP pattern was only tested on tropical cyclones occurring in that basin. The WP pattern uses two action centers for the measurement: the first is located over the Kamchatka Peninsula (60°N, 155°E) and the second is located over the western subtropical North Pacific (30°N, 155°E); (Wallace and Gutzler 1981; Linkin and Nigam 2008).

The pattern is known to have a strong negative correlation between the two action centers in a north-south dipole pattern with a high-pressure center over the Kamchatka Peninsula in the north and a low-pressure center in the warmer climate found over the western subtropical North Pacific. According to Choi and Moon (2012), strong positive and negative WP anomalies are associated with zonal (east-west) and meridional (north-south) variations in the location of the East Asian jet stream. These fluctuations of the jet stream have a significant impact on the climate of East Asia. The positive WP phase is associated with a ridge pattern southeast of Japan bringing above-average temperatures over the subtropical western North Pacific in winter and

9

spring seasons. In the negative phase, a trough in the jet stream is associated with below-average temperatures over the northern extents of the Asian continent (Choi and Moon 2012).

The WP teleconnection has also been found to have an impact on tropical cyclones occurring in the western North Pacific basin. An extensive study by Choi and Moon (2012) found that more tropical cyclones tend to occur in the positive WP phase than in the negative WP phase. The authors attributed the change in tropical cyclone frequency to anomalous warm SSTs in the western North Pacific during the positive WP phase and stronger convective activity (Choi and Moon 2012). Furthermore, it was found that the WP pattern has an influence on the track of western North Pacific tropical cyclones. During the positive WP phase, a strengthened cyclonic flow in the subtropical western North Pacific and an anticyclonic flow in the middle latitudes creates enhanced southeasterly winds around Korea, Japan, and the East China Sea that put the region at an increased risk for tropical cyclones steering in that direction (Choi and Moon 2012).

Building upon the research of Wallace and Gutzler (1981), Linkin and Nigam (2008), and Choi and Moon (2012), this study uses the WP teleconnection as an explanatory variable to identify alterations in tropical cyclone geography in the western North Pacific basin under various conditions. Any correlation found between the WP teleconnection phase and variance in the latitude and/or longitude of tropical cyclogenesis furthers the body of knowledge on the subject that can be used for forecasting and climatological research.

El Niño Southern Oscillation (ENSO)

The most widely known and well-studied teleconnection pattern in the world is the ENSO. According to Stoner et al. (2009), the ENSO is a coupled atmospheric-oceanic cycle that was first noted by English physicist Sir Gilbert Walker in 1923 (Walker 1923). The phenomenon is caused by a breakdown of the easterly trade winds called the Southern Oscillation (SO) and

has a ripple effect on many climatic cycles (Hanley, Bourassa, O'Brien, Smith, and Spade 2003).

The weakening trade winds allow warm surface water normally concentrated in the western

Pacific to backflow eastward toward the coast of Peru, resulting in warmer than normal ocean

waters in the eastern Pacific Ocean. Increased heat from the warm water, in turn, causes

amplified condensation and heat transfer into the troposphere (McPhaden 2002; Figure 2.2). The

excessive heat is responsible for multiple altered circulation patterns in the atmosphere that

impact normal climate with extremes like droughts, floods, and modifications in tropical cyclone

activity. La Niña events, on the other hand, typically occur the year after El Niño events and

have just the opposite effect of El Niño. Here, colder than normal ocean temperatures are

situated in the tropical east Pacific and have the ability to suppress tropical cyclone activity and

manipulate other weather patterns in the region (Hanley et al. 2003). ENSO also drives global

wind patterns that interact with many other atmospheric processes and other teleconnection

patterns like the PNA, PDO, and MJO (Zhang and Gottschalck 2002; Mantua 2002; Wang,

Kumar, and Xue 2012).
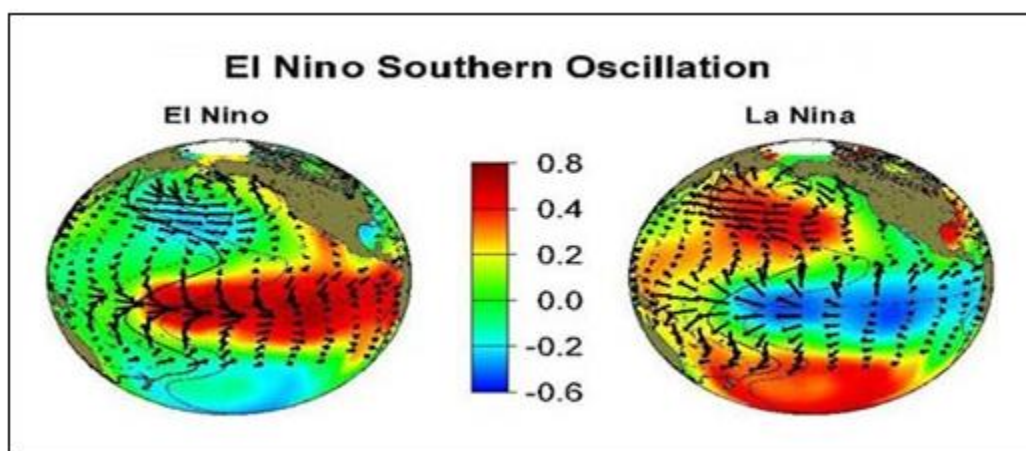
Figure 2.2. SST anomalies associated with El Niño and La Niña phases of ENSO.
(Source: www.intellicast.com/Community/Content.aspx?ref=rss&a=151)

Multiple indices are used to measure the phase of ENSO using different methodologies and reference points. In this research, the Southern Oscillation Index (SOI) and the Multivariate ENSO Index (MEI) were used to measure the phase of ENSO as positive, neutral, or negative. The SOI is a standardized index used to measure the state of the SO, the atmospheric pressure component of ENSO, over the Pacific Ocean. The SOI measures the difference in sea level pressure (SLP) between Tahiti, French Polynesia and Darwin, Australia. El Niño (La Niña) events have a negative (positive) index value and are associated with above-average (below-average) SLP at Darwin and below average (above average) SLP at Tahiti (Hanley et al. 2003).

The MEI, originally proposed by Wolter and Timlin (1993), is calculated using six weighted variables over the tropical Pacific Ocean. The variables used in the MEI calculation are: SLP, SST, zonal and meridional components of the surface wind, surface air temperature, and a cloudiness fraction of the sky (Hanley et al. 2003). Opposite of the SOI, El Niño (La Niña) measurements using the MEI have a positive (negative) value (Oliver 2010). Both indices are used in this study in order to provide a more comprehensive analysis of the ENSO in relation to tropical cyclone geography in the Pacific Ocean.

In the Eastern North Pacific, the amplified SST near Mexico and Baja, California increases the likelihood of tropical storm systems and major tropical cyclones (Stoner et al. 2009). It has also been found that tropical cyclones have a tendency to travel further northward and westward in El Niño conditions since the pool of warm ocean water is larger than normal (McPhaden 2002). The influence of ENSO in the western North Pacific basin has also been studied by multiple scientists. El Niño (La Niña) events in the western North Pacific have been correlated with increased (decreased) accumulated cyclone energy, suggesting that the teleconnection pattern has an influence on the strength of tropical cyclones in the basin

12

(Camargo and Sobel 2005). However, El Niño events have not been significantly correlated with increased frequency of tropical cyclone genesis (Whitney and Hobgood 1997; Camargo, Emanuel, and Sobel 2007). It has also been found that ENSO has an influence on the location of tropical cyclogenesis in the western North Pacific. Chia and Ropelewski (2002) studied the relationship between ENSO and western North Pacific tropical cyclones for the years 1979-1999. They found that during El Niño events, tropical cyclones tended to form to the southeast of the mean center genesis position and northwest of the mean center in La Niña conditions. The variability in tropical cyclogenesis location is attributed to upper level vertical wind shear, SSTs, the position of the monsoon (East Asian) trough, and the position of the western Pacific subtropical high-pressure center (Chia and Ropelewski 2002; Camargo et al. 2007). The methodology of this study is similar to that of Chia and Ropelewski; however, the study period will be much larger (1979-2016) and contain more tropical cyclones.

Pacific Decadal Oscillation (PDO)

The phenomenon known today as the PDO was first studied and identified by fisheries scientist Steven Hare in 1996. During extensive research on the atmospheric factors associated with variability in the salmon fishing industry, Hare concluded that a decadal alteration in Pacific climatology (the PDO) was linked with ecological impacts affecting the Alaskan salmon population (Hare 1996; Mantua, Hare, Zhang, Wallace, and Francis 1997). The PDO is defined as an anomalous phasing warm/cool pattern of SST variability over the tropical and northeast Pacific Ocean (Mantua et al. 1997; Wang et al. 2012). The PDO index, defined by SST anomalies in the Pacific northward of 20°N latitude, is representative of warm (positive) phases and cool (negative) phases (Stoner et al. 2009). The PDO is often compared to ENSO with warm

(El Niño-like) and cold (La Niña-like) phases, however, some primary distinctions do exist between the two teleconnections:

> Three main characteristics distinguish PDO from El Niño/Southern Oscillation (ENSO): first, 20th century PDO events persisted for 20–30 years, while typical ENSO events persisted for 6 to 18 months; second, the climatic fingerprints of the PDO are most visible in the North Pacific/North American sector, while secondary signatures exist in the tropics, while the opposite is true for ENSO; and third, the mechanisms that cause PDO are not currently known, while causes for ENSO are relatively well understood (Mantua 2002).

The warm (positive) phase of the PDO is distinguished by anomalously high SSTs in the tropical central and tropical eastern Pacific and along the North American coast (Figure 2.3). The warm PDO phase is also characteristic of cooler than normal SSTs in the central North Pacific near the semi-permanent Aleutian low-pressure center and in the western North Pacific. During this period, the Aleutian low is stronger than normal and counterclockwise flow is enhanced causing stronger than normal westerly winds in the eastern North Pacific (Mantua 2002). The positive (warm) phase of the PDO tends to weaken the cold California Current that is normally found along the western coast of North America as the warmer than normal water in the central tropical Pacific propagates northward with the enhanced counterclockwise flow (Rohli and Vega 2012). Alternatively, the cold (negative) phase of the PDO is characterized by colder than normal SSTs along the coast of North and Central America, with a core of above average SSTs in the central and western North Pacific (Rohli and Vega 2012).

Since the PDO is strongly correlated with ENSO, the two teleconnection patterns can alter the normal patterns found in previous studies. Depending on what phase the two

teleconnections are in they can cancel each other out or amplify climatic variability (Mantua et al. 1997; Rohli and Vega 2012). For example, if a warm phase of the PDO syncs with an El Niño event, the impact on the tropical pacific can be enhanced by above average SSTs and atmospheric wind patterns. Similarly, the synchronization of the two teleconnections can impact tropical cyclone development (Mantua 2002).
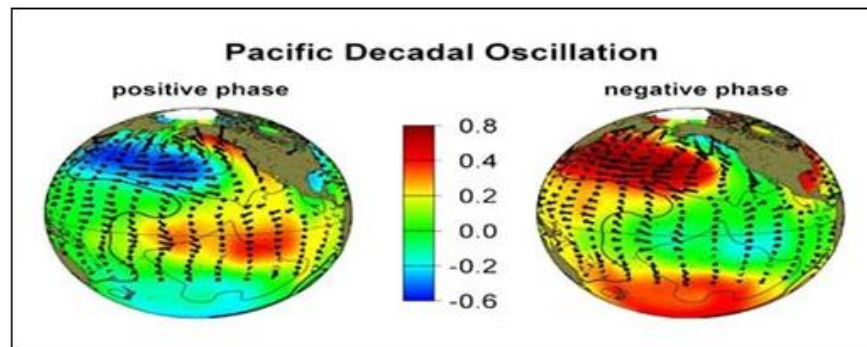
Figure 2.3. SST anomalies associated with warm (positive) and cold (negative) PDO phases. (Source: www.intellicast.com/Community/Content.aspx?ref=rss&a=151)

Madden-Julian Oscillation (MJO)

The fifth teleconnection pattern used in this study is the MJO. The MJO has a much shorter period of influence than large-scale climatic events like ENSO and is often called the 30-60 Day Oscillation. The teleconnection is characterized as an eastward-moving disturbance of clouds, rain, winds, and alternating pressure that travels the tropics and disrupt normal atmospheric patterns. The MJO acts in a dipole pattern; it has a period of strong low-level convection with stormy weather and increased rainfall, as well as a period of calm weather with suppressed rainfall (Figure 2.4). The intensity (amplitude) and geographic location (phase) of the MJO are measured using a real-time multivariate MJO (RMM) index developed by Matthew Wheeler and Harry Hendon (2004). Their mathematical methods measure the cloudiness amount, as well as upper and lower level winds to determine MJO amplitude and intensity. As the MJO

moves eastward across the globe, its geographic location is plotted using a phase-space diagram

with the amplitude of the corresponding event (Figure 2.5; Wheeler and Hendon 2004).
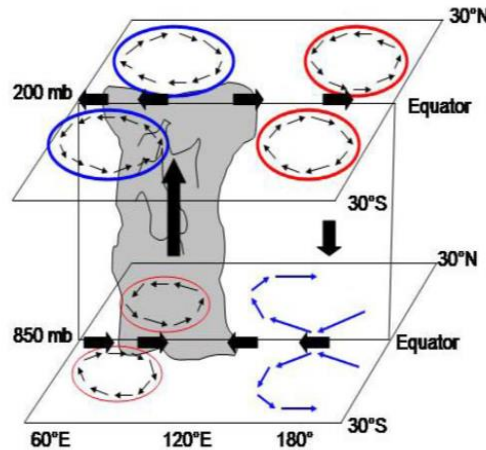
Figure 2.4. Schematic of the vertical structure of the MJO
(Source: Rui and Wang 1990).

It has been proven (Maloney and Hartman 2001; Higgins and Shi 2001; Zhang 2013) that

the MJO has an influence on tropical cyclones forming in the eastern Pacific Ocean basin, and

especially influences the strongest storms forming in the region (Gottschalck, Kousky, Higgins,

and L'Heureux n.d.). As the strong convective center of the MJO moves across the Pacific from

west to east, the low-pressure center creates a westerly wind anomaly in and behind the enhanced

convection area with an area of high pressure to the east. In the upper levels, anticyclonic flow

develops atop the area of convection, creating more upper level divergence and allowing the

system to grow vertically as wind shear is reduced (Gottschalck et al. n.d.). According to

Maloney and Hartman (2000), over twice as many named tropical storms occur during the

equatorial westerly anomalies than the easterly anomalies. Furthermore, major tropical cyclones

are over four times more frequent during the western phase of the MJO (Maloney and Hartman

2000). In addition to the works of Gottschalck et al., Maloney and Hartman, and many other

16

researchers, this study aims to provide further information about the influence of the MJO on tropical cyclogenesis geography in the eastern and western North Pacific basins.
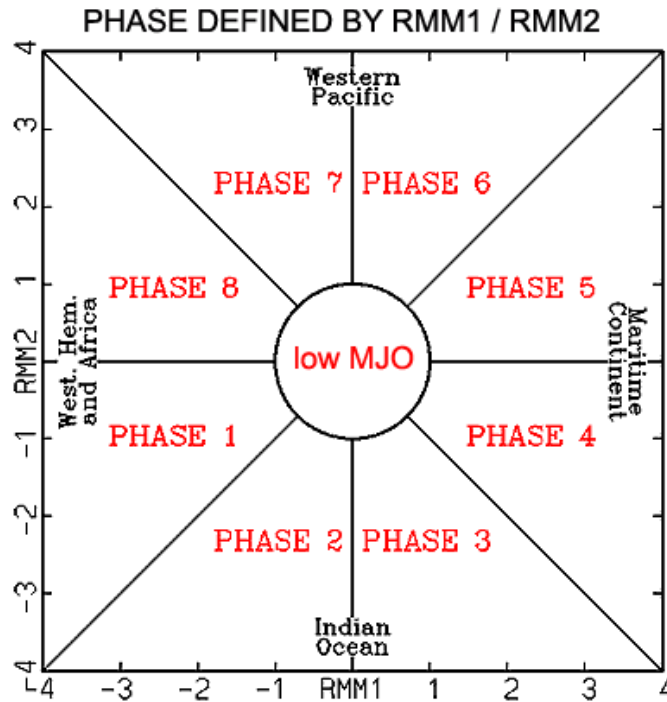
Figure 2.5. MJO phase-space diagram used by Wheeler and Hendon (2004) to monitor and model the phase and amplitude of the MJO.
(Source: http://la.climatologie.free.fr/MJO/MJO1-english.htm)

Quasi-Biennial Oscillation (QBO)

Research that lead to the eventual establishment of the QBO dates back to the late 1800s to early 1900s. During the 19th century before the use of modern data instruments, it was assumed that stratospheric winds in the tropics blew from east to west. One of the earliest hypotheses of stratospheric wind direction was reinforced by the eruption of the Krakatua volcano in 1883. On August 27, the volcano erupted and littered tropical locations around the globe with volcanic debris over the next two weeks as the dust cloud gradually spread from east to west. Thereafter, equatorial stratospheric winds became known as Krakatua easterlies

(Baldwin et al. 2001). Contrarily, scientist A. Berson collected data in 1908 from weather balloons launched in Africa that recorded winds blowing from west to east (westerlies) in similar atmospheric heights as the Krakatua easterlies; now known as the Berson westerlies (Baldwin et al. 2001). The inconsistency in wind direction lead to research by scientists like Reed and Rogers (1962) who used wind data for multiple years to study the reversal of wind patterns and draw conclusions.

The pattern known today as the QBO was first identified by Richard Reed and Veryard and Ebdon in 1960. The QBO is defined by oscillations in easterly (negative) and westerly (positive) zonal winds in the tropical stratosphere with a mean time span of 26-28 months. The wind patterns develop in the lower stratosphere typically near 30-50 mb and propagate downward over time at a general rate of 1 kilometer (0.6 mi) per month, taking roughly 13 months to complete each interval and 26 months for the complete cycle (Figure 2.6; Baldwin et al. 2001). The highest velocity winds are found in the lower stratosphere around 30 km (98,000ft) and weaken as they move toward the tropopause where the wind patterns eventually die and the next (opposite) phase is generated. Further research has shown that the westerly phase of the QBO is more regular than the easterly phase, but the easterly phase is nearly twice as strong and tends to have a longer duration (Baldwin et al. 2001; Rohli and Vega 2012).

The QBO has been linked to variations in tropical cyclone activity in multiple ocean basins including the Pacific (Angell et al. 1969). The westerly phase of the QBO is associated with heightened tropical cyclone activity and more intense tropical cyclones while the opposite is true for the easterly phase (Ho, Kim, Jeong, and Son 2009; Rohli and Vega 2012). The QBO has also been found to impact tropical cyclone tracks in the western North Pacific depending on the teleconnection phase. According to a study by Ho et al. (2009), more tropical cyclones approach

the East China Sea during the westerly phase of the QBO and shift toward the east coast of Japan

during the easterly phase. Building upon the cited research above, this thesis project correlates

the influence of the QBO with tropical cyclogenesis geography in the eastern and western North

Pacific basins.
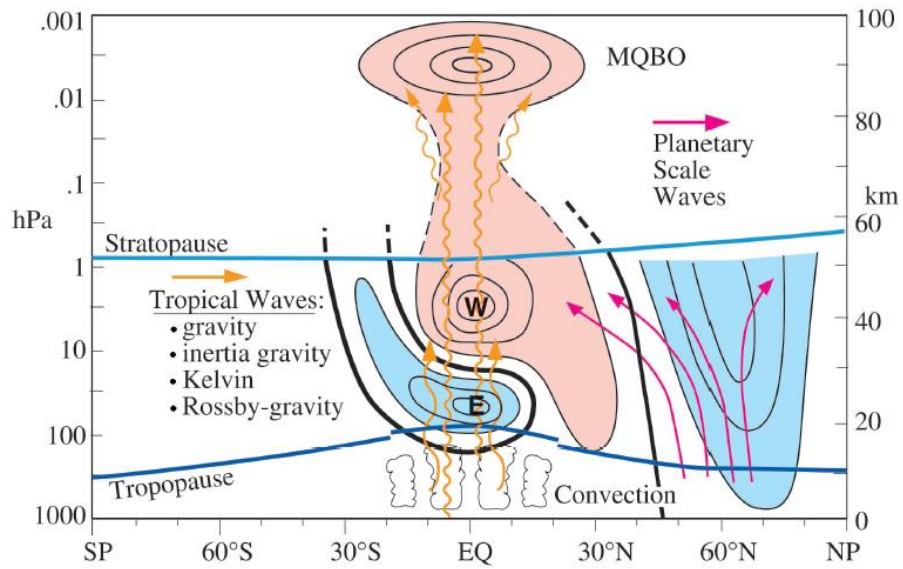
Figure 2.6. Model of the QBO in the vertical structure of the atmosphere.
(Source: Baldwin et al. 2001)

CHAPTER 3
METHODOLOGY

3.1 Areas of Interest

The study area for this thesis research covers the entire North Pacific Ocean. The North Pacific Ocean basin is defined as the portion of the Pacific Ocean that is contained within the Northern Hemisphere between the equator and the Arctic Ocean. For the purposes of this study, the North Pacific Ocean was further divided into two portions; the eastern North Pacific basin and the western North Pacific basin. By splitting the Pacific into two portions, the author could independently analyze teleconnection impacts on both eastern and western Pacific tropical cyclones.

Eastern North Pacific Basin

The eastern North Pacific Ocean was considered the area from the 180th parallel (also known as the antimeridian or International Date Line) eastward to the coast of Northern and Central America. The northern extent meets the Bering Sea at the Aleutian Islands while the southern extent of the eastern North Pacific basin is 0° latitude (Equator), with most tropical cyclone activity taking place between 5° and 20°N (Figure 3.1.1). All tropical cyclones occurring in this region were considered an eastern North Pacific event.
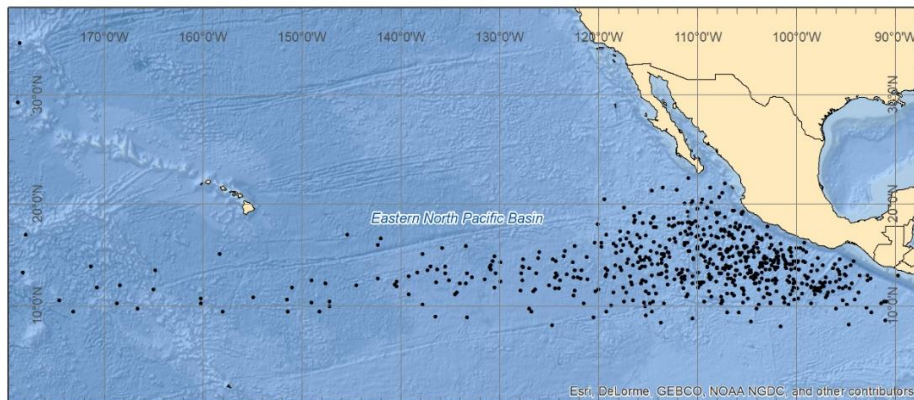
Figure 3.1.1. Map portraying cyclogenesis locations and the eastern
North Pacific basin for the purposes of this study.

Western North Pacific Basin

Like the eastern North Pacific, the western North Pacific basin spans from the equator at 0° latitude to the Aleutian Islands and the Russian Far East at its northernmost extent before meeting the Bering Sea. For the purposes of this study, the western North Pacific basin was considered the area encompassed from the antimeridian (180°) westward to roughly 100°E (Figure 3.1.2). Here, the western North Pacific meets numerous marginal seas such as the Sea of Japan and the Philippine Sea near the Asian mainland and surrounding islands.
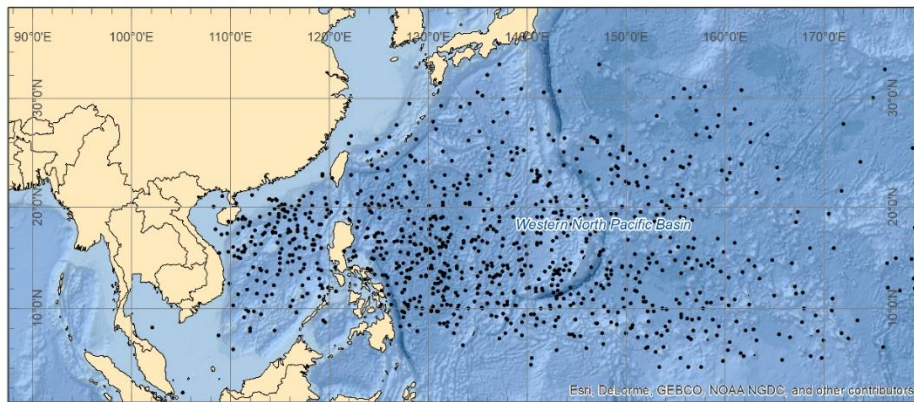
Figure 3.1.2. Map portraying cyclogenesis locations and the western North Pacific basin for the purposes of this study.

3.2 Dependent Variables

Eastern North Pacific Basin

Since climatological data cover large areas and are well-funded by government entities, all data used in this study is secondary. Eastern North Pacific tropical cyclone records were obtained from the National Hurricane Center (NHC) "Best Track" NE/NC Pacific HURDAT2 database (NHC Data Archive 2017). The database contains measurements for storm parameters every six hours from the first time of observation until the storm system dissipates and becomes non-threatening. The measured parameters include atmospheric pressure, wind speed, latitude, longitude, and storm status. Although the HURDAT2 database contained data for storms ranging

from tropical disturbances to major tropical cyclones, only storm systems reaching tropical storm status or greater were used in this study. By doing so, it allowed an emphasis to be placed on storms that had the right atmospheric conditions for intensification to occur. The dataset was also limited to storm systems that only developed during the official eastern North Pacific hurricane season from May 15th to November 30th. In total, 626 tropical cyclone records were used for analysis from the period 1979-2016.

Western North Pacific Basin

Western North Pacific tropical cyclone data was collected from the Japan Meteorological Agency Regional Specialized Meteorological Center (RSMC) Tokyo Typhoon Center "Best Track" dataset (Japan Meteorological Agency RSMC Best Track Data 2017). Similar to the NHC Best Track dataset, the western North Pacific data was available in six-hour intervals with information regarding storm status, latitude, longitude, central atmospheric pressure, and wind speed. Tropical cyclones occurring in the western North Pacific in all months were used in this study since the western Pacific tropical cyclone season lasts year-round. However, most storms tend to occur from May to October much like the eastern North Pacific. In total, 964 tropical cyclones were used in the analysis from the period 1979-2016.

3.3 Independent (Explanatory) Variables

Teleconnection data was also collected from secondary sources since the data cover a very large geographic area and the analysis period spans 37 years. A major data source for this project was the NOAA Earth Systems Research Laboratory (ESRL) Physical Sciences Division archive. The ESRL portal provides data for over 30 atmospheric and oceanic time series on a monthly basis. For use in this study, the PNA, SOI, MEI, QBO, and WP teleconnection data

were obtained from the NOAA ESRL online data portal on a monthly time scale from 1979 to 2016 (NOAA ESRL Data 2017). The PDO index was obtained from NOAA's National Centers for Environmental Information (NCEI) website (NOAA NCEI Data 2017). Furthermore, MJO data was collected from the Australian Bureau of Meteorology (Australian Bureau of Meteorology Data 2017). Both the phase and the amplitude of the MJO were used in this study for the period 1979-2016 since both were indicators of the strength and location of MJO. All seven teleconnection indices were not tested on the whole study area since they have varying areas of impact around the globe.

Eastern North Pacific Basin

In the eastern North Pacific basin, the PNA, SOI, MEI, MJO and QBO indices were tested independently to find out if they had a significant correlation with variance in the geography of tropical cyclogenesis. For the period 1979-2016, the index value for each teleconnection pattern was recorded for use in the statistical analysis explained in Sections 3.4 and 3.5. For the MJO, both the phase and amplitude were tested in the eastern North Pacific basin. The WP teleconnection index was not tested on this portion of the Pacific basin because it does not have a significant presence in the eastern North Pacific study area (Choi and Moon 2012).

Western North Pacific Basin

Like the eastern Pacific, six teleconnection patterns were also tested for significance in the western Pacific basin. The WP, SOI, MEI, MJO, and QBO teleconnection indices were examined. Again, both the MJO phase and amplitude were used for testing in the western North Pacific basin. The PNA teleconnection was not tested for correlation with western Pacific tropical cyclogenesis since the teleconnection does not exert a strong influence in the study area.

23

3.4 Analytical Methods and Tools

To analyze the relationship between the geography of tropical cyclogenesis and each teleconnection index, tropical cyclone data was compiled for both the eastern and western Pacific basins. For each basin, the tropical cyclones were sorted by the year, month, and day that the storm first reached at least tropical storm strength (minimum 34 knots). Next, each tropical cyclone record was paired with the corresponding teleconnection index value for the same time that the storm occurred. All data was organized and analyzed using Microsoft Excel.

The key pieces of data for the purposes of this study were the latitude and longitude coordinates that represent where in the Pacific Ocean the storm first became at least tropical storm strength. The geographic coordinates were used to statistically analyze how the geography of cyclogenesis changes with the fluctuation of each teleconnection using a simple linear regression model. For each of the seven independent variables (x), two regression models were created that tested the significance of the variables against the dependent variable latitude (y^1) and dependent variable longitude (y^2).

$$\text{Latitude } (y^1) = \beta_0 + \beta_1 x + \varepsilon$$

$$\text{Longitude } (y^2) = \beta_0 + \beta_1 x + \varepsilon$$

In this simple linear regression equation, β_0 is the intercept, β_1 is the coefficient of x (independent variable), and ε is the error for the regression analysis.

Furthermore, the data trends between the dependent and independent variables were spatially analyzed by creating cluster density maps for each teleconnection analysis. ArcMap 10.5.1, a geographic information system (GIS) software developed by Environmental Systems Research Institute (ESRI), was used to map each of the 626 tropical cyclones in the eastern North Pacific, and 964 tropical cyclones in the western North Pacific by their geographic

coordinates. The latitude and longitude coordinates were displayed on the map using the World Geodetic System 1984 (WGS84) geographic coordinate system and Mercator Projection.

For mapping purposes, the mean, standard deviation, lower boundary, and upper boundary were calculated for each teleconnection index. Using the standard deviation, three phases were assigned for each teleconnection index; a "normal" neutral phase that lies within one standard deviation of the mean, a positive phase that is greater than one standard deviation from the mean, and a negative phase that is more than one standard deviation less than the mean. Using this methodology, tropical cyclones were mapped as either positive, neutral, or negative according to the corresponding teleconnection index value that was present whenever the storm first reached the tropical storm strength threshold. The methodology for MJO phase was dissimilar since it is a simple integer and not a variable index.

After mapping each tropical cyclone according to the phase of the independent teleconnection index, a point density analysis was conducted on each of the three phases. A kernel density function in ESRI ArcMap was used to calculate the density of tropical cyclones per unit area in both the eastern and western North Pacific basins. The kernel density analysis method is based on an algorithm created by B.W Silverman (1986) that calculates the density per unit area of input point features around each raster cell in the output dataset. The analysis uses a circular neighborhood around each input point with a standard search radius (bandwidth) to fit a smooth, tapered surface over the output raster. Using this methodology, patterns of tropical cyclogenesis cluster density shifting under each phase was analyzed.

3.5 Teleconnection Combination Analysis

An additional portion of this study was devoted to a multiple linear regression analysis that tested combinations of each teleconnection phase and the effect that each combination has

on Pacific cyclogenesis geography. The combination analysis method provides a more comprehensive investigation of how the teleconnection patterns interact with each other in their respective areas of dominance. For both the eastern and western Pacific, 16 teleconnection combinations were tested. For each basin, the four most statistically significant results from the simple linear regression independent teleconnection analysis were used for the combination multiple regression analysis to condense the results. Although the SOI and MEI were both highly significant independent variables, only the SOI was used for the combination analysis since both indices are representative of the ENSO. The SOI, PDO, MJO phase, and QBO were the four most statistically significant indices in both the eastern and western Pacific basins.

$$\text{Latitude } (y^1) = \beta_0 + \beta_1 x_1 + \beta_2 x_2 + \beta_3 x_3 + \beta_4 x_4 + \varepsilon$$

$$\text{Longitude } (y^2) = \beta_0 + \beta_1 x_1 + \beta_2 x_2 + \beta_3 x_3 + \beta_4 x_4 + \varepsilon$$

In this multiple linear regression equation, β_0 is the intercept, $\beta_{(1-4)}$ are the coefficients of $x_{(1-4)}$ (each of the four independent variables), and ε is the error for the regression analysis. The multiple regression analysis was performed for both the latitude (y^1) and longitude (y^2) dependent variables of tropical cyclogenesis location in the eastern and western North Pacific basins.

CHAPTER 4
RESULTS

4.1 Eastern North Pacific Basin Independent Analysis

The simple linear regression analysis produced statistically significant results at the 95% ($p < .05$) confidence interval or greater for five of the six teleconnection indices evaluated in the eastern North Pacific basin for the period 1979-2016 (SOI, MEI, PDO, MJO phase, and QBO). Table 4.1.1 contains a summary of the linear regression results with P-values, R^2 values, and coefficients for each of the six teleconnection indices tested in the eastern North Pacific basin. Three of the teleconnection indices (SOI, MEI, PDO) produced results that were considered highly statistically significant ($p < .001$) for association with latitudinal shifting; furthermore, MJO phase and QBO were found to be significant indicators of latitude at the $p < .05$ level.

Only three teleconnection indices were found to have a statistically significant correlation with variance in longitude. The SOI had the highest significance at $p < .001$, with MEI and MJO phase also showing significant results at the $p < .05$ level. PNA and MJO amplitude were not found to have a significant impact on cyclogenesis latitude or longitude in the eastern North Pacific basin. In general, the teleconnections indices explained more of the variance in tropical cyclone latitude than longitude in the eastern North Pacific basin during the study period.

Teleconnection	PNA	SOI	MEI	PDO	MJO Phase	MJO Amp.	QBO
Latitude							
R^2	n/s	0.033	0.049	0.028	0.010	n/s	0.007
p-value	n/s	0001	0.001	0.001	0.014	n/s	0.034
Coefficient	n/s	0.384	-0.704	-0.409	-0.108	n/s	-0.017
Longitude							
R^2	n/s	0.024	0.008	n/s	0.010	n/s	n/s
p-value	n/s	0.001	0.030	n/s	0.012	n/s	n/s
Coefficient	n/s	-1.726	1.458	n/s	-0.588	n/s	n/s

Table 4.1.1. Eastern North Pacific basin linear regression analysis results for each of the six teleconnection indices including R^2, coefficient, and P-value for latitude and longitude. Variables labeled (n/s) were not significant.

Table 4.1.2 contains further information on the mean and standard deviation, as well as upper and lower boundaries for each of the six teleconnection indices. Each tropical cyclone was paired with the corresponding teleconnection index value measured at the time that the storm first reached tropical storm status. In conjunction with the latitude and longitude parameters for each tropical cyclone tested in the eastern North Pacific, these values were used to categorize all 626 tropical cyclones as occurring in the positive, neutral, or negative phase for point density mapping purposes. The point density maps provide a visual representation of the linear regression results through the use of geospatial analysis.

Teleconnection	PNA	SOI	MEI	PDO	MJO Phase	MJO Amp.	QBO
Mean	-0.03	-0.18	0.48	-0.26	n/a	1.15	-4.76
Std. Deviation	0.98	1.33	0.89	1.15	n/a	0.57	14.21
Upper Boundary	0.95	1.15	1.37	0.89	n/a	1.71	9.44
Lower Boundary	-1.01	-1.52	-0.41	-1.41	n/a	0.58	-18.97
Upper Extreme	2.87	3.7	3.01	2.41	n/a	3.11	15.62
Lower Extreme	-2.61	-4.3	-2.02	-3.05	n/a	0.10	-29.05

Table 4.1.2. Mean, standard deviation, upper and lower boundaries, and upper and lower extremes for each of the six teleconnection indices analyzed in the eastern North Pacific basin. MJO phase is not applicable since it uses an integer (1-8) to indicate phase.

Pacific North American (PNA)

The PNA teleconnection was the only independent variable that did not explain a statistically significant amount of the variance in tropical cyclogenesis latitude or longitude in the eastern North Pacific basin. According to the R^2 value, the PNA accounted for less than 1% of the variance in latitude and longitude. In the neutral PNA phase (-1.01 to 0.95), tropical cyclones tended to cluster heavily between 10°N to 20°N latitude and 100°W to 110°W longitude (Figure 4.1.1). In the eastern North Pacific, this 10°x10° block is the hotspot for major tropical cyclone activity as the formation trend can be examined throughout the study with minor variation in the neutral phase.

Some variation in cyclogenesis cluster shifting can be seen between the positive and negative phase of the PNA in Figure 4.1.1. During the positive PNA phase (0.96 to 2.87), the average longitude for cyclogenesis decreases from the mean (112.01°W) to 109°W. During the negative PNA phase (-1.02 to -2.61), the average longitude increases to 113.66°W. The slight shift in clustering can be examined in Figure 4.1.1 and signals a weak negative correlation between the PNA and cyclogenesis longitude. However, the point density map seems to accurately portray the regression results that the PNA does not significantly impact the latitude or longitude of tropical cyclogenesis.

Figure 4.1.1. Point density maps for eastern North Pacific tropical cyclogenesis during positive, neutral, and negative phases of the PNA based on standard deviation from the mean.

Southern Oscillation Index (SOI)

The SOI, an indicator of ENSO, had among the highest significance in association with tropical cyclone cluster shifting in the eastern North Pacific basin. According to the R^2 value, the SOI explained slightly greater than 3% of the variance ($R^2 = .033$) in cyclogenesis latitude and nearly 2.5% ($R^2 = .024$) of the variance in longitude for the study period in the eastern North Pacific. Both regression analyses were significant at the $p < .001$ level. By examining Figure 4.1.2, cluster shifting is evident under positive, neutral, and negative phases.

In general, cyclogenesis occurred at higher latitudes during the positive SOI phase (1.16 to 3.7) than in the negative phase (-1.53 to -4.3). These findings support the positive relationship that was found during the regression analysis where cyclogenesis latitude increased as SOI increased. Based on Figure 4.1.2, tropical cyclogenesis clusters can be seen between 11°N and approximately 21°N latitude during the positive (La Niña) phase. Comparatively, tropical cyclogenesis during the negative (El Niño) phase occurred at lower latitudes with clustering occurring between 11°N to 16°N latitude.

The phase of SOI also influenced tropical cyclogenesis longitude for the period 1979-2016 in the eastern North Pacific basin. In the positive phase, cyclogenesis was highly clustered between 98°W to 112°W along the western coast of Mexico. However, during the negative phase, tropical cyclones were much more likely to form further west of those boundaries. By examining Figure 4.1.2, clusters of tropical cyclogenesis in the negative SOI phase can be found from 94°W to 116°W longitude. Furthermore, there are noticeably more tropical cyclones forming west of 130°W during the negative SOI phase. These findings support the negative relationship found by the regression analysis where longitude decreases (shifts east) as SOI increases.

31

Figure 4.1.2. Point density maps for eastern North Pacific tropical cyclogenesis during positive, neutral, and negative phases of the SOI based on standard deviation from the mean.

Multivariate El Niño Southern Oscillation Index (MEI)

The second indicator of the ENSO used in this study is the MEI. Like the SOI, this index also explained a significant portion of the variance in tropical cyclone latitude and longitude for the study period in the eastern North Pacific basin. The MEI explained 4.9% of the variance (R^2 = .049) in latitude of tropical cyclogenesis (an increase of 1.6% over the SOI) with a significance of p < .001. However, MEI was not as effective at explaining variance in cyclogenesis longitude as the SOI; it explained less than 1% of the variance (R^2 = .008) with p = .03.

The cluster density maps for SOI (Figure 4.1.2) and MEI (Figure 4.1.3) show many similarities. For MEI, the positive (negative) phase is indicative of the El Niño (La Niña) phase of the ENSO; opposite of SOI. Like the cluster density map of the negative SOI phase, the MEI positive phase (1.38 to 3.01) in Figure 4.1.3 shows clusters of cyclogenesis further south, east, and west than in the negative MEI phase. In terms of latitude, the densest clustering occurred between 10°to 16°N during the positive phase and 12° to 21°N during the negative phase (-0.42 to -2.02). The point density maps support the findings of the linear regression analysis. MEI and latitude have a negative correlation according to the coefficient; as MEI increases, tropical cyclogenesis latitude tends to decrease.

On the other hand, MEI and cyclogenesis longitude have a positive correlation; as MEI increases, longitude also tends to increase. In the positive phase, tropical cyclogenesis occurs further west (greater longitude) than in the negative phase. Overall, tropical cyclogenesis tended to migrate south and west as MEI increased during El Niño-like conditions. Likewise, cyclogenesis shifts north and east closer to the coast of Mexico as MEI decreases in La Niña-like conditions. As explained with SOI, this pattern is due to the nature of ENSO and will be further discussed in Chapter 5.
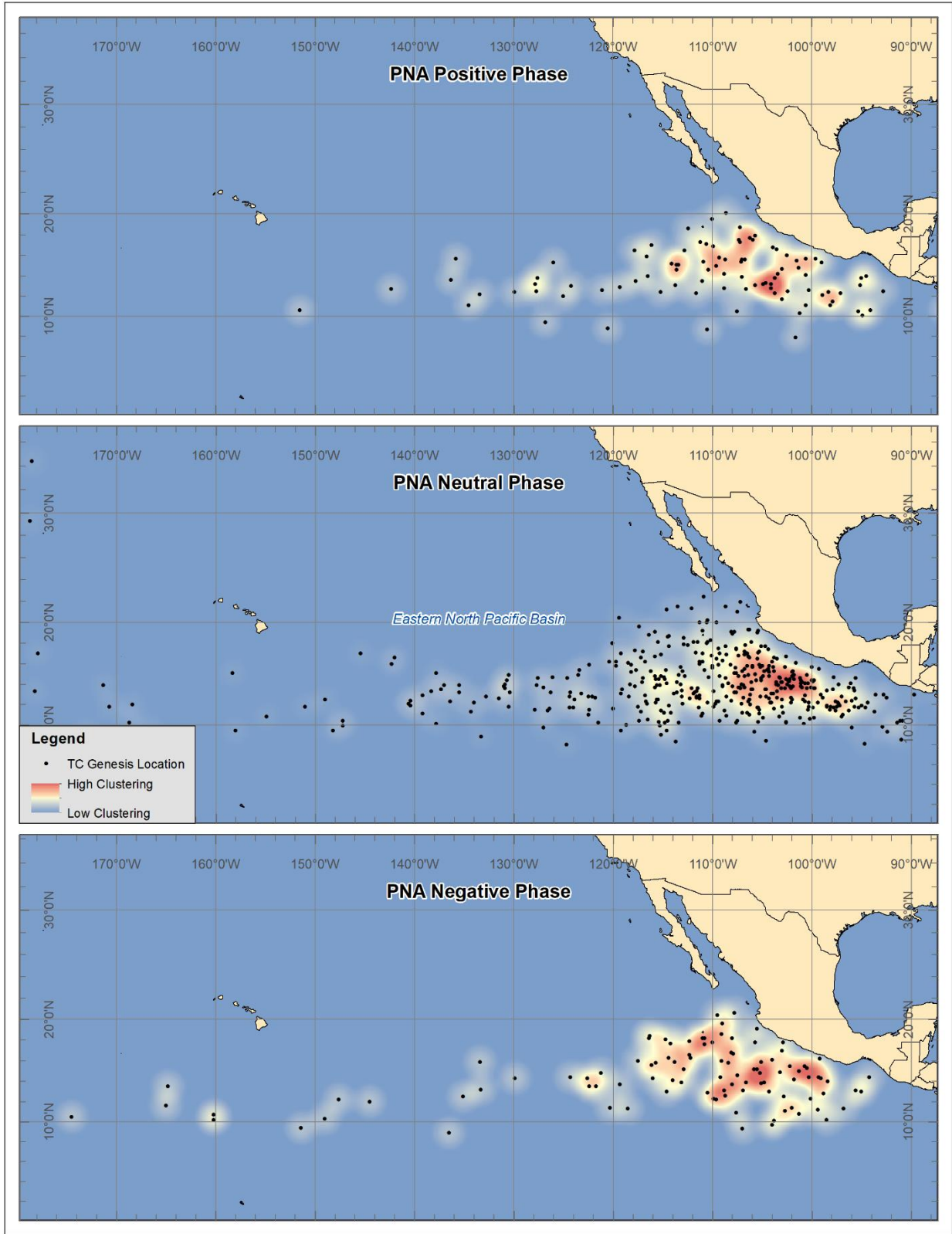
Figure 4.1.3. Point density maps for eastern North Pacific tropical cyclogenesis during positive, neutral, and negative phases of the MEI based on standard deviation from the mean.

Pacific Decadal Oscillation (PDO)

The linear regression results for the PDO were found to be statistically significant for only changes in tropical cyclogenesis latitude. During the study period 1979-2016, the PDO explained nearly 3% of the variance (R^2 = .028) in tropical cyclogenesis latitude in the eastern North Pacific basin at the p > .001 (99%) confidence interval. The PDO did not have a statistically significant correlation with changes in cyclogenesis longitude during the study period.

Figure 4.1.4 spatially depicts the influence of the PDO on tropical cyclogenesis in the eastern North Pacific basin. In the positive phase (0.90 to 2.41), tropical cyclogenesis clustered between 10° to 16°N latitude and largely between 94° to 108°W longitude. The negative phase (-1.42 to -3.05) depicts much different results with heavy clustering between 12° to 22°N latitude and 99° to 116°W longitude. Overall, the spatial analysis results support the negative correlation found between the PDO and cyclogenesis latitude in the linear regression analysis. As the PDO increases (decreases) from the mean, cyclogenesis latitude generally decreases (increases). In the positive phase, the average cyclogenesis latitude decreased to 13.16°N from 14.03°N in the neutral phase. Furthermore, the average latitude increased in the negative PDO phase to 14.74°N, further solidifying the negative correlation. Some small clusters also occur west of the main bodies in both the positive and negative phase.
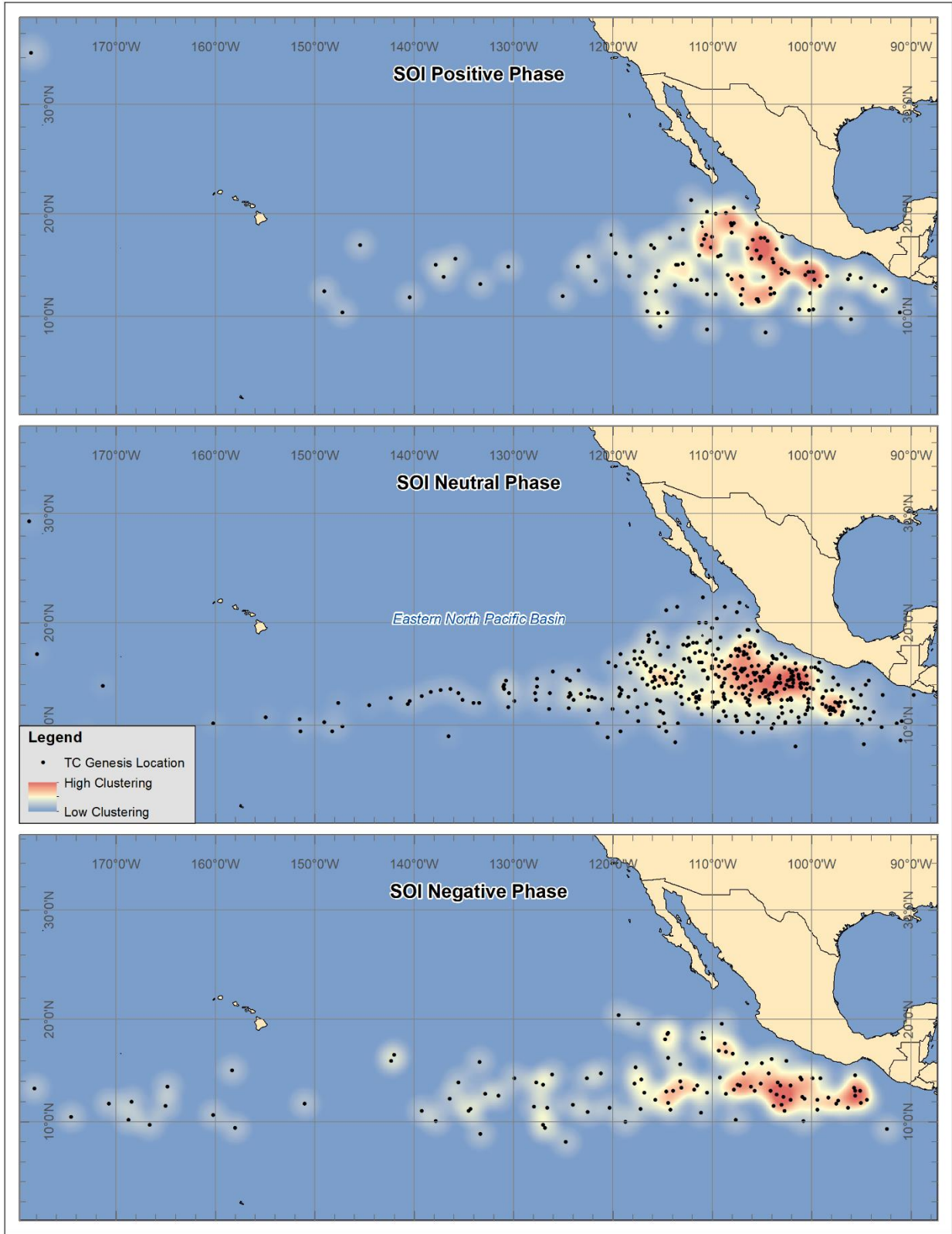
Figure 4.1.4. Point density maps for eastern North Pacific tropical cyclogenesis during positive, neutral, and negative phases of the PDO based on standard deviation from the mean.

Madden-Julian Oscillation (MJO)

Both the MJO phase and amplitude were regressed against the latitude and longitude of eastern North Pacific tropical cyclones occurring between 1979-2016. For this period, MJO amplitude did not produce statistically significant results during linear regression testing. However, MJO phase did prove to be a statistically significant determinant of tropical cyclone latitude and longitude. MJO phase explained about 1% of the variance in latitude and longitude ($R^2 = .01$) and was significant at the 95% confidence interval with p-values of $p = .014$ and $p = .011$, respectively. Figure 4.1.5 and 4.1.6 depict the clustering of tropical cyclones in each of the eight phases of MJO. Unlike the other teleconnection indices, this method was used to display and analyze the results for MJO phase since it is not recorded by positive/negative index range like MJO amplitude and could not be separated into a positive, neutral, and negative phase using the mean and standard deviation.

The nature of MJO as an eastward-moving atmospheric disturbance creates a much different pattern of tropical cyclogenesis clustering than the other teleconnection patterns in this study. Although the other teleconnections fluctuate between phases, they do not travel around the globe in 30 to 60 days like the MJO, influencing tropical rainfall, wind patterns, atmospheric pressure, and tropical cyclones. Figures 4.1.5 and 4.1.6 display some of the dramatic effects of MJO on tropical cyclogenesis. In addition, Table 4.1.3 provides information on average cyclogenesis latitude and the number of tropical cyclones occurring in each phase of the MJO.

In phase 1, tropical cyclogenesis is amplified and tends to cluster tightly along the coast of Mexico between 11° to 18°N latitude. For the study period 1979-2016, 135 tropical cyclones reached at least tropical storm status under phase 1 of MJO; the most tropical cyclone activity of any phase. Likewise, phase 2 also shows signs of amplified tropical cyclogenesis. For the

specified study period, 95 tropical cyclones intensified to at least tropical storm status under

phase 2 of MJO; tied with phase 8 for second most tropical cyclone activity of any MJO phase.

Clustering for phase 2 changed slightly from phase 1 with more defined clusters forming west of

the main body. These results support the linear regression analysis that found a negative

correlation between MJO phase and longitude; as MJO phase increased, cyclogenesis was more

likely to occur at higher longitudes (further west). Tropical cyclogenesis still tended to occur

close to the southwestern coast of Mexico in the eastern North Pacific basin in phase 2.

MJO phases 3-7 were characterized by much less tropical cyclone activity and less

intense clustering. During phase 3, cyclogenesis seems to occur most frequently in a more

southerly pattern than in phases 1 and 2. Clustering in phase 4 is more sporadic but occurs

further west than in previous phases. Phases 5-7 are also quite sporadic with no clear spatial

pattern developments. Phase 8, however, displays a spike in cyclogenesis activity and similar

clustering patterns to those found in phases 1 and 2.

Figure 4.1.7 presents the results of the cluster analysis for the positive, neutral, and

negative phases of MJO amplitude. MJO amplitude did not produce statistically significant

results for explaining variance in cyclogenesis latitude or longitude in the eastern North Pacific

basin. Figure 4.1.7 supports those findings; no clear spatial patterns of cyclogenesis clustering

emerged by comparing the positive, neutral, and negative phases of MJO amplitude.

MJO Phase	1	2	3	4	5	6	7	8
Avg. Lat. °N	14.57	14.27	13.55	13.69	14.65	13.56	13.41	13.91
Num. TCs	135	95	58	54	51	70	68	95

Table 4.1.3. MJO phase, average cyclogenesis latitude, and number of tropical cyclones
reaching at least tropical storm strength in the eastern North Pacific.
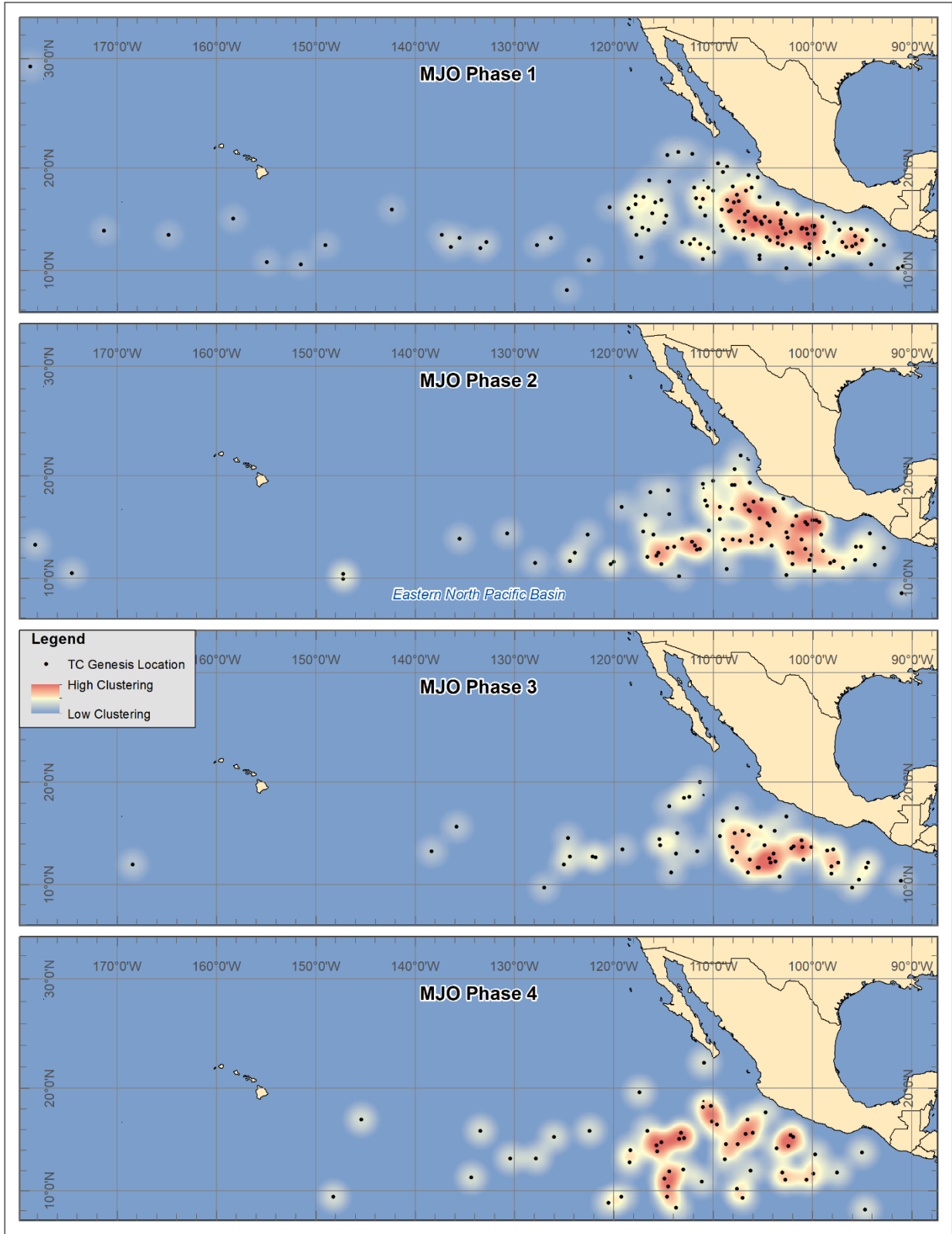
Figure 4.1.5. Point density maps for eastern North Pacific tropical cyclogenesis during phases 1-4 of the MJO.

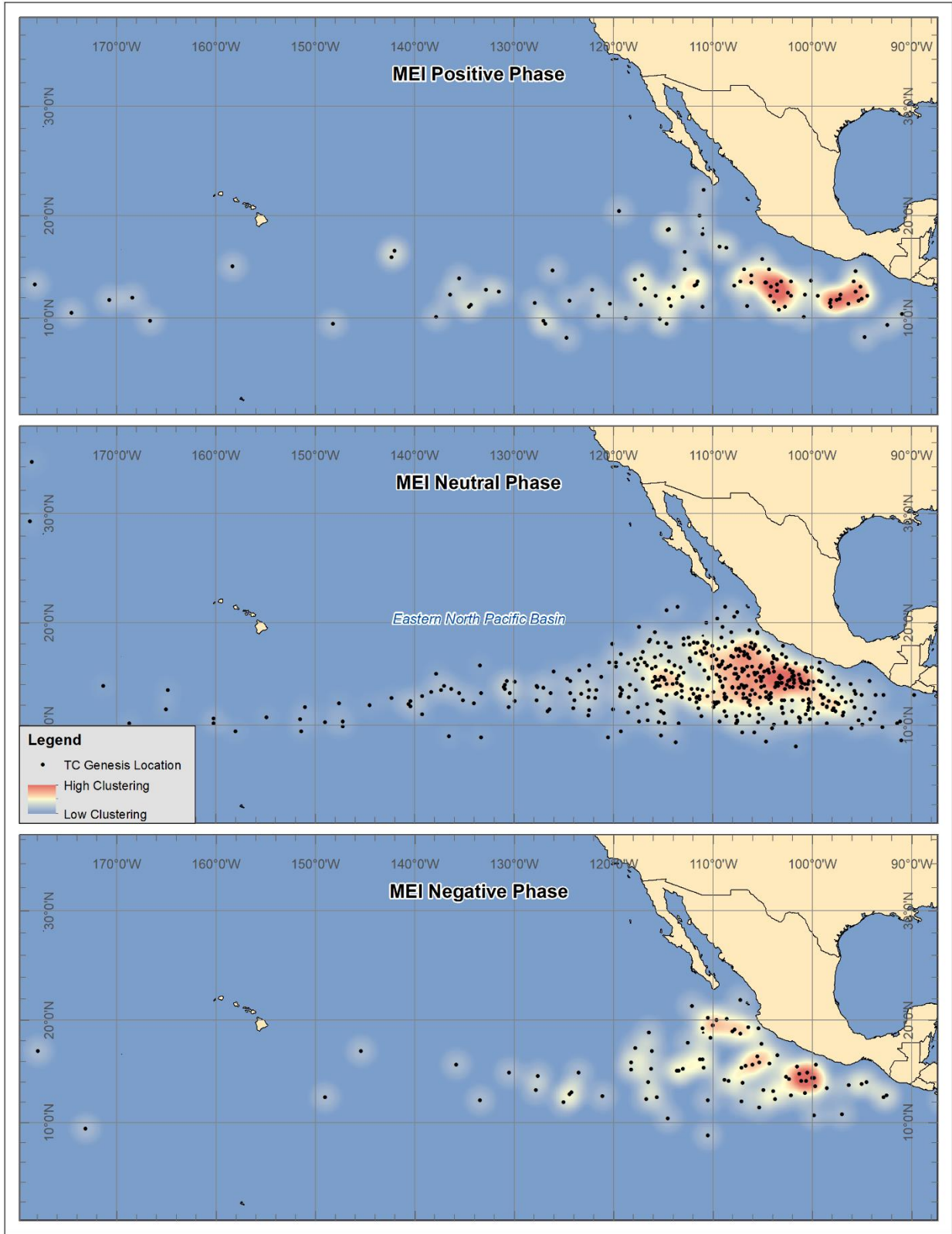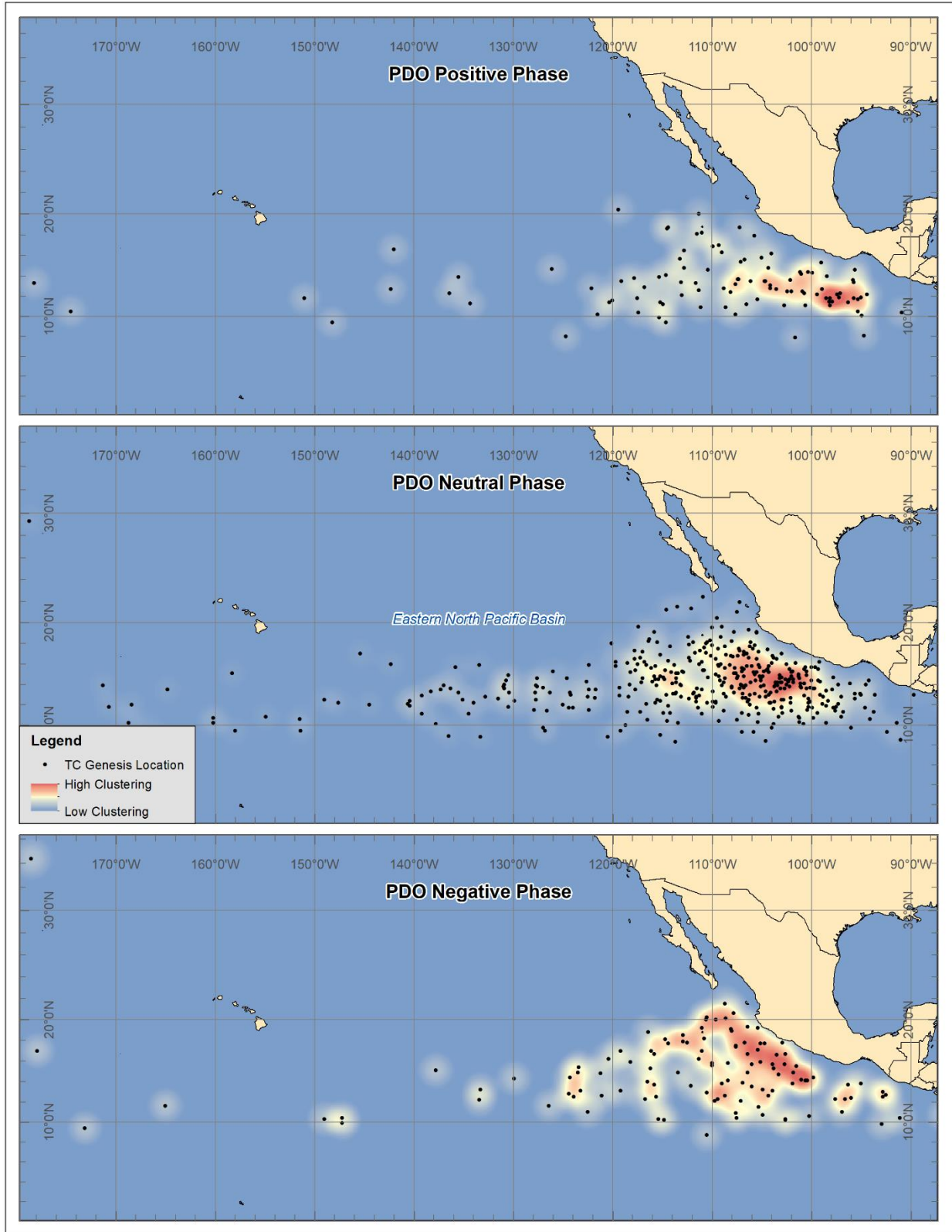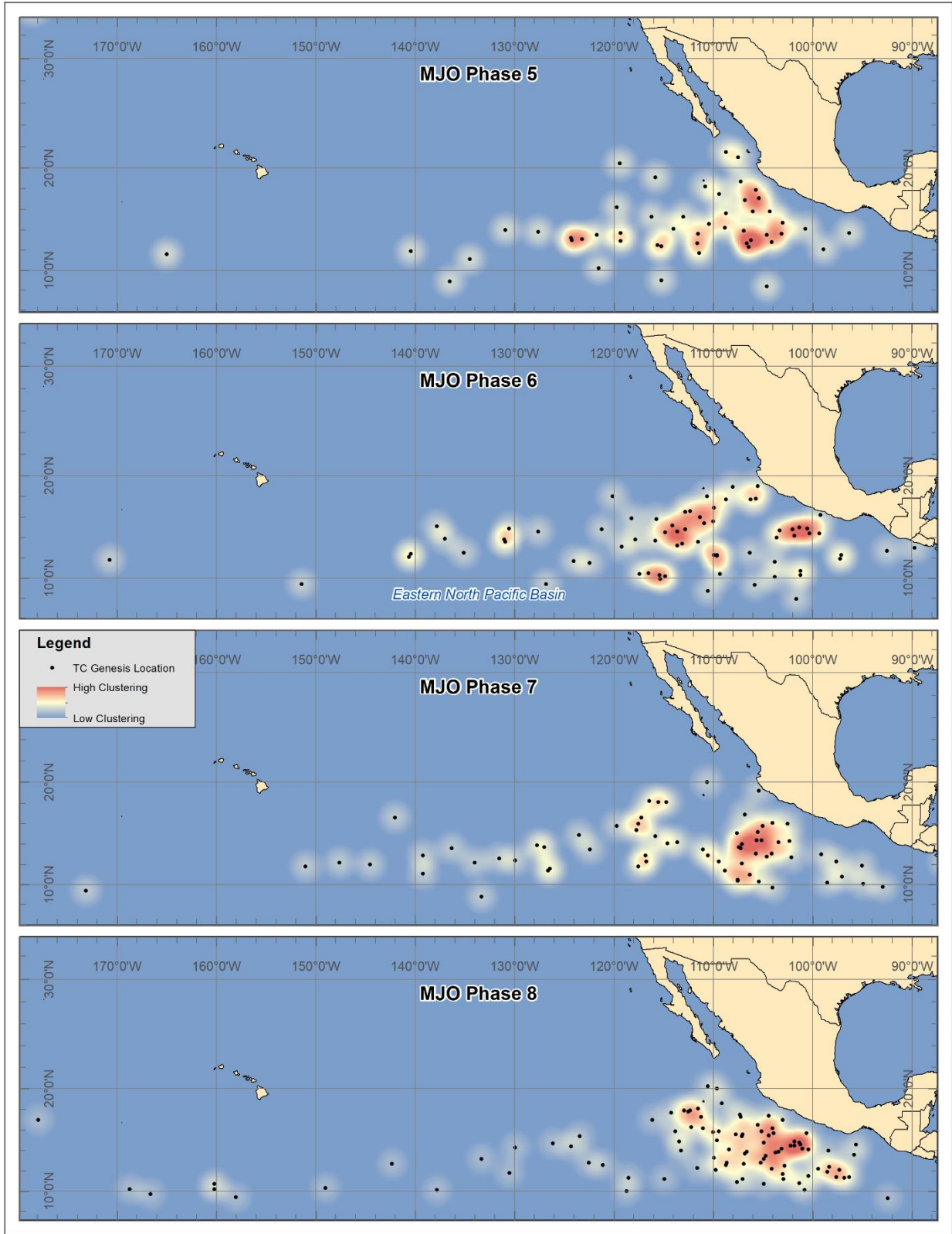**Figure 4.1.6.** Point density maps for eastern North Pacific tropical cyclogenesis during phases 5-8 of the MJO.
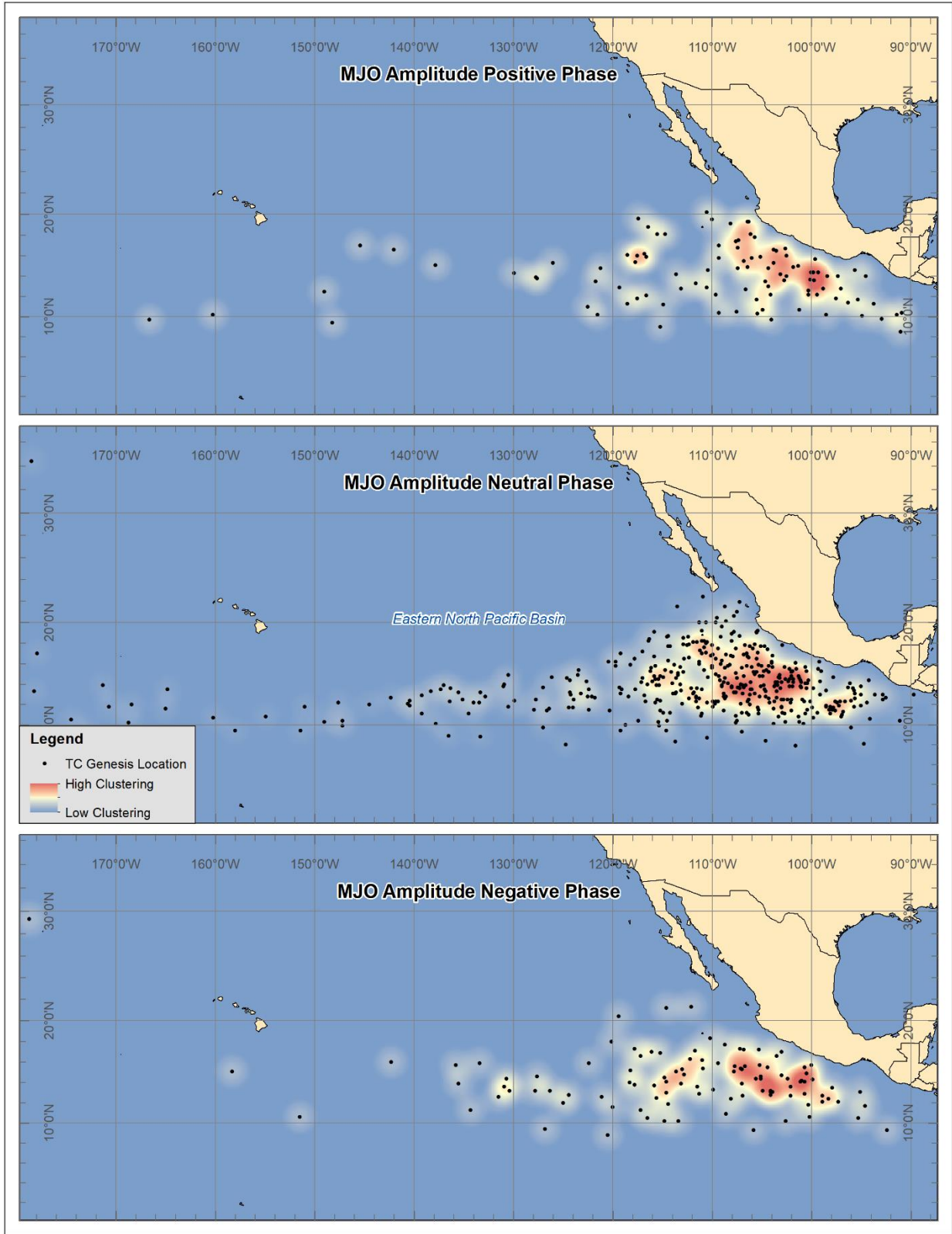
Figure 4.1.7. Point density maps for eastern North Pacific tropical cyclogenesis during positive, neutral, and negative phases of MJO amplitude based on standard deviation from the mean.

Quasi-Biennial Oscillation (QBO)

The QBO teleconnection pattern was found to be a statistically significant explanatory variable of cyclogenesis latitude for eastern North Pacific tropical cyclones. However, the teleconnection only explained less than 1% of the variance ($R^2 = .007$) in latitude for the 626 tropical cyclones used in this study. The teleconnection was statistically significant at the 95% confidence interval with the p-value of .034 when regressed against cyclogenesis latitude. The QBO was not found to be a significant explanatory variable of longitude for the same study area and period.

Figure 4.1.8 provides a visual representation of the graphical analysis results. In the neutral phase (-18.97 to 9.44), the average cyclogenesis latitude is 13.79°N. During the positive phase (9.45 to 15.62), tropical cyclogenesis is highly clustered between 11° to 19°N and the average latitude increases slightly to 14.07°N. In the negative phase (-18.98 to -29.05), the highly clustered cyclogenesis area tends to shift north between 13° to 19°N and has an average cyclogenesis latitude of 14.48°N. Although the average latitude of cyclogenesis increased in both the positive and negative phase and the QBO only explained < 1% of the variance in cyclogenesis latitude, the overall findings support the weak negative correlation found during the linear regression analysis. Cyclogenesis latitude had a greater increase during the negative phase than during the positive phase.
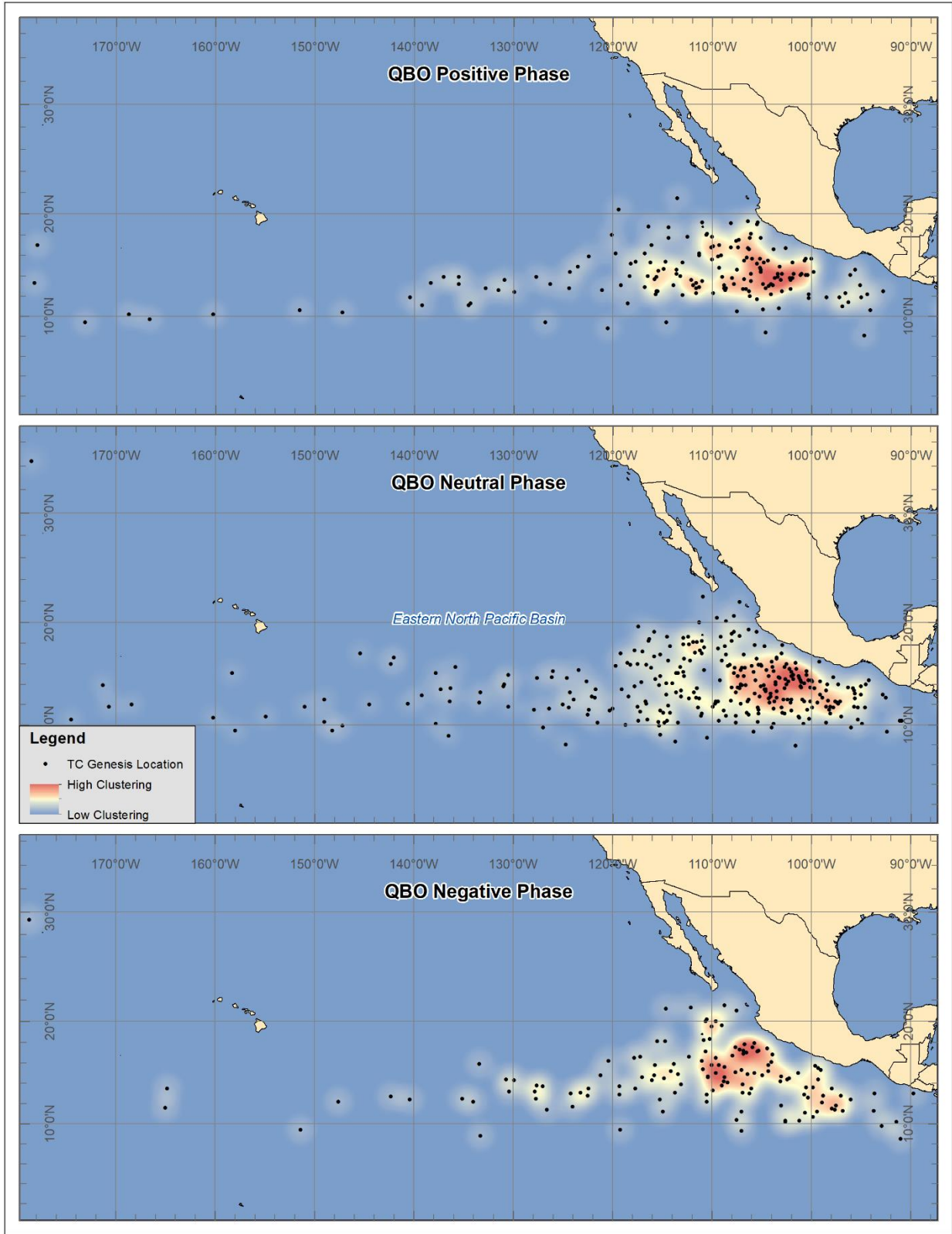
Figure 4.1.8. Point density maps for eastern North Pacific tropical cyclogenesis during positive, neutral, and negative phases of the QBO based on standard deviation from the mean.

43

4.2 Eastern North Pacific Basin Combination Analysis

The four most significant explanatory variables during independent testing in the eastern North Pacific basin were the SOI, PDO, MJO, and QBO indices. Therefore, they were used in the multiple regression analysis to test the effect of numerous teleconnection phase combinations on the geography of Pacific tropical cyclogenesis. Sixteen teleconnection combinations were tested using a positive and negative phase for each of the four indices. For MJO phase, 1-4 was considered positive while 5-8 was considered negative for the purposes of this study. The results of the analysis are displayed in Table 4.2.1 with a combination reference number, p-value, and R^2 value for both latitude and longitude analyses. Furthermore, a series of maps containing the cluster density analysis results are located in the appendix for each combination. In cases where any of the four teleconnection values were equal to zero whenever a tropical cyclone occurred, the record was not analyzed since the analysis was based on values < 0 and > 0. In total, eight of the 626 tropical cyclone records were excluded from analysis because of index values equal to zero.

Overall, the teleconnection combinations were inefficient at explaining variance in cyclogenesis latitude or longitude for the eastern North Pacific basin. Only three combinations had a strong enough relationship with the dependent variable (latitude) to explain a significant portion of the variance at the 95% (p < .05) confidence interval. Furthermore, only one of the sixteen combinations tested significant at the same confidence interval for correlation with longitude variance. Many of the other combinations that were not significant at the 95% confidence interval were considered marginal since they produced low p-values and high R^2 values but fell short of the p < .05 threshold.

Combo #	SOI	PDO	MJO	QBO	Latitude p-value	Latitude R^2	Longitude p-value	Longitude R^2	Num. of Storms
1	+	-	+	-	0.973	0.010	0.135	0.126	56
2	-	+	-	+	0.044	0.360	0.482	0.146	26
3	+	+	-	-	0.598	0.068	0.607	0.067	43
4	-	-	+	+	0.849	0.050	0.603	0.096	31
5	+	-	-	-	0.869	0.029	0.375	0.096	46
6	-	+	+	+	0.765	0.037	0.402	0.079	53
7	+	-	-	+	0.797	0.073	0.581	0.122	26
8	-	+	+	-	0.515	0.084	0.493	0.088	41
9	+	+	+	-	0.041	0.208	0.118	0.157	47
10	-	-	-	+	0.060	0.304	0.014	0.393	29
11	+	+	-	+	0.892	0.097	0.895	0.095	15
12	-	-	+	-	0.068	0.155	0.344	0.083	56
13	+	-	+	+	0.196	0.121	0.290	0.100	51
14	-	+	-	-	0.049	0.273	0.918	0.031	34
15	+	+	+	+	0.364	0.327	0.374	0.322	15
16	-	-	-	-	0.738	0.043	0.076	0.171	49

Table 4.2.1. Results of the eastern North Pacific teleconnection combination analysis. Values in black were found to be statistically significant at the 95% confidence interval.

Combination #2 (SOI - PDO + MJO - QBO +) most effectively explained variance in latitude (36%) with a p-value = .044 and R^2 value of .36. From 1979-2016, 26 tropical cyclones reached at least tropical storm status under these conditions; less than the average value of 38 tropical cyclones in each grouping. Combination #1 is the inverse of combination #2 (SOI + PDO - MJO + QBO -); 56 tropical cyclones occurred under these conditions for the same time period. However, the teleconnection combination did not effectively explain the variance in latitude or longitude for combination #1. The other two combinations that produced statistically significant results for the latitude test were #9 (SOI + PDO + MJO + QBO -) and #14 (SOI - PDO + MJO - QBO -). The multiple regression analysis produced p-values of .041 and .049, respectively, with R^2 values of .208 and .273. Combination #9 contained an above average number of tropical cyclones (47) while combination #14 was slightly below average with 34.

Combination #10 (SOI - PDO - MJO - QBO +) was the only group to explain a statistically significant portion of the variance in cyclogenesis longitude. The multiple regression analysis had a p-value of .014 with an R^2 of .393. During these conditions, only 29 storms reached at least tropical cyclone strength from 1979-2016. Adversely, 47 tropical cyclones meeting the same threshold occurred during the inverse combination (#9; SOI +PDO + MJO + QBO -), but the multiple regression analysis failed to explain a significant portion of the variance in longitude for this combination.

4.3 Western North Pacific Basin Independent Analysis

Like the eastern North Pacific basin, six teleconnection indices were also independently tested in the western North Pacific for the study period 1979-2016. The WP, SOI, MEI, PDO, MJO, and QBO teleconnection indices were used as independent variables in the simple linear regression analysis, with all of them producing statistically significant results at the 95% confidence interval or greater except the WP teleconnection pattern. Table 4.3.1 presents the results of the linear regression analyses for each independent variable against the latitude and longitude of western North Pacific tropical cyclones.

Five of the teleconnection indices were found to have a statistically significant correlation with variation in latitude in the western North Pacific basin (SOI, MEI, PDO, MJO, QBO). Of the five significant variables, four of them were considered highly significant at the 99% (p < .001) confidence interval (SOI, MEI, PDO, MJO phase). The QBO was found to be significant at the 95% (p < .05) confidence interval.

The simple linear regression analysis produced less significant results for association with longitude shifting of tropical cyclones. Three of the six teleconnection indices were found

to be significant indicators of variance in tropical cyclogenesis longitude (SOI, MEI, and PDO). The WP, MJO, and QBO did not exert a strong enough impact to be considered statistically significant for shifting in western Pacific tropical cyclogenesis longitude. Similar to the eastern North Pacific, the independent variables tended to explain more of the variance in tropical cyclogenesis latitude than longitude.

Teleconnection	WP	SOI	MEI	PDO	MJO Phase	MJO Amp.	QBO
Latitude							
R^2	n/s	0.033	0.034	0.042	0.019	0.007	0.006
p-value	n/s	0.001	0.001	0.001	0.001	0.012	0.013
Coefficient	n/s	0.737	-1.170	-1.006	-0.351	-0.750	-0.032
Longitude							
R^2	n/s	0.046	0.036	0.014	n/s	n/s	n/s
p-value	n/s	0.001	0.001	0.001	n/s	n/s	n/s
Coefficient	n/s	-2.529	3.478	1.666	n/s	n/s	n/s

Table 4.3.1. Western North Pacific basin linear regression analysis results for each of the six teleconnection indices including R^2, coefficient, and P-value for latitude and longitude. Variables labeled (n/s) were not significant.

In addition to the linear regression analysis statistics, the mean and standard deviation were calculated for each of the teleconnection indices. Table 4.3.2 contains the results for each of these parameters as well as the upper and lower boundaries and upper and lower extremes for each teleconnection index. The upper (lower) boundary was calculated by adding (subtracting) the standard deviation to (from) the mean. The upper and lower extremes are the highest and lowest value the teleconnection index reached during the study period 1979-2016. Like the eastern North Pacific, these values were used to classify all 964 tropical cyclones into a positive, neutral, or negative phase based on the index value of each teleconnection index for cluster density mapping purposes. MJO phase was mapped by each of the eight phases.

Teleconnection	WP	SOI	MEI	PDO	MJO Phase	MJO Amp.	QBO
Mean	0.024	-0.071	0.316	-0.300	n/a	1.185	-4.632
Std. Deviation	1.038	1.400	0.896	1.153	n/a	0.608	14.109
Upper Boundary	1.062	1.329	1.212	0.854	n/a	1.793	9.476
Lower Boundary	-1.014	-1.471	-0.581	-1.453	n/a	0.577	-18.741
Upper Extreme	3.290	4.100	3.005	2.410	n/a	3.328	15.620
Lower Extreme	-2.530	-4.700	-2.019	-3.050	n/a	4.47E-02	-29.550

Table 4.3.2. Mean, standard deviation, upper and lower boundaries, and upper and lower extremes for each of the six teleconnection indices analyzed in the western North Pacific basin. MJO phase is not applicable since it uses an integer (1-8) to indicate phase.

West Pacific (WP)

The WP teleconnection pattern was the only independent variable tested in the western North Pacific basin that did not produce any statistically significant results at the 95% confidence interval threshold. The linear regression analysis results show that the WP teleconnection index failed to explain a significant portion of the variance in tropical cyclogenesis latitude or longitude. The R^2 value for both regression analyses were less than .01 (1%). Figure 4.3.1 shows the results of the cluster density analysis performed using the WP pattern and corresponding cyclogenesis locations. In the neutral phase (-1.014 to 1.062), large clusters of tropical cyclogenesis can be found off the eastern coast of the Phillipines and in the South China Sea between the Phillipines and the Asian mainland. Although cyclogenesis in the western North Pacific occurred all the way to the easternmost extent at 180°, the clustering is largely concentrated west of 140°E. In terms of latitude, most cyclones are concentrated between 8°N to 22°N.

Outside of the neutral phase, the spatial analysis seems to support the findings of the linear regression analyses. No clear patterns of cluster shifting are evident as the teleconnection fluctuates into the positive and negative phase. Clustering in the positive phase tended to be more

48

concentrated east of the Phillipines than in the negative WP phase. Only three major clusters of cyclogenesis activity can be seen in the negative phase; one in the South China Sea, another cluster east of the Phillipines, and another just east of 140°E.

Figure 4.3.1. Point density maps for western North Pacific tropical cyclogenesis during positive, neutral, and negative phases of the WP based on standard deviation from the mean.

Southern Oscillation Index (SOI)

The SOI performed well in the simple linear regression analysis when tested against both latitude and longitude of western North Pacific cyclogenesis locations. Both parameters yielded results at the 99% confidence interval with p-values of less than .001 when regressed against the SOI. The teleconnection index explained slightly better than 3% of the variance in tropical cyclogenesis latitude for the study period with an R^2 value of .033. For longitude, the SOI accounted for 4.6% of the variance ($R^2 = .046$); the highest R^2 value of the six teleconnection patterns tested in the western Pacific basin.

Figure 4.3.2 displays the results of the spatial analysis performed using the positive, neutral, and negative phases of SOI calculated from the mean and standard deviation. The cluster density analysis generally supports the findings of the linear regression with cluster shifting occurring in each phase. In the neutral phase (-1.471 to 1.329), a familiar cyclogenesis hotspot can be found off the eastern coast of the Philippines and in the South China Sea; similar to the neutral phase of the WP teleconnection pattern in Figure 4.3.1. However, in the positive SOI phase (1.33 to 4.1), cyclogenesis latitude tends to shift north with more clustering occurring north of 20°N latitude. Similarly, cyclogenesis latitude tended to retract toward the equator in the negative phase (-1.472 to -4.7) of the SOI with most clustering occurring south of 18°N. These results correspond with the positive correlation found between the SOI and latitude in the linear regression analysis. As the SOI increases (decreases), cyclogenesis latitude also tends to increase (decrease).

The clustering patterns found in Figure 4.3.2 during the positive phase of the SOI versus the negative phase are quite drastic. In addition to latitude shifting as the SOI fluctuates, there are also noticeable changes in the longitude component of cyclogenesis geography. In the positive

phase, most clustering occurred west of 144°E longitude with large, dense clusters. In fact, 116 of the 154 (75.3%) mapped cyclogenesis locations in the positive phase occurred west of 140°E longitude. By comparison, only 73 of the 168 (43.4%) locations mapped in the negative SOI phase occurred west of 140°E latitude. The density of cyclogenesis points in the negative phase are much less concentrated. There is a strong shift in cyclogenesis to the east during the negative phase that corresponds with the negative correlation found between the SOI and cyclogenesis longitude. As the SOI increased, cyclogenesis longitude tended to decrease from the mean (shift west). Likewise, as the SOI decreased, cyclogenesis longitude tended to increase from the mean (shift east). The negative correlation is supported by the cluster density analysis found in Figure 4.3.2.
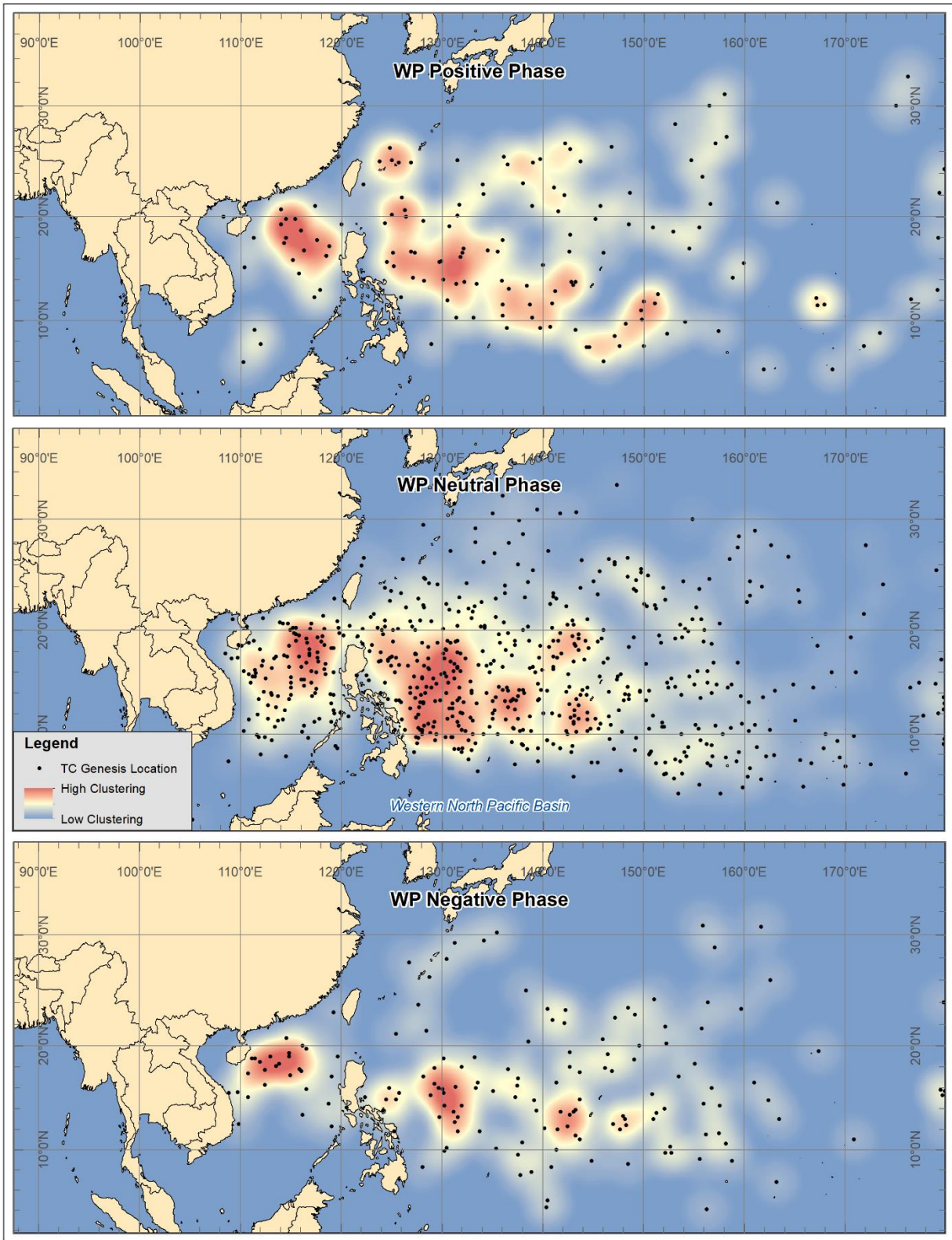
Figure 4.3.2. Point density maps for western North Pacific tropical cyclogenesis during positive, neutral, and negative phases of the SOI based on standard deviation from the mean.

53

Multivariate El Niño Southern Oscillation Index (MEI)

The second indicator of the ENSO teleconnection pattern, MEI, also produced statistically significant results during linear regressing. The independent variable explained 3.4% of the variance in cyclogenesis latitude and 3.6% of the variance in longitude with R^2 values of .034 and .036, respectively. Like the SOI, the MEI is indicative of the ENSO pattern; however, the two indices work opposite of each other. As previously stated in the eastern Pacific results section, the positive phase of SOI indicates La Niña-like conditions whereas the negative MEI phase indicates similar ENSO conditions. Likewise, negative SOI values indicate El Niño conditions while positive MEI values signal the same pattern.

By comparing Figures 4.3.2 and 4.3.3, similar patterns of cluster shifting can be examined in opposing index phases. The positive phase of MEI (1.213 to 3.005) has a pattern similar to that of the negative SOI phase in Figure 4.3.2 where cyclogenesis clustering tended to shift south in comparison to the other two phases. During the positive phase of MEI, the average latitude was 14.12°N. In the negative MEI phase (-0.582 to -2.019), the average latitude of cyclogenesis drastically changes to 18.17°N as intense clusters form off the eastern coast of the Philippines and mainland Asia. These figures are representative of the negative relationship found between the MEI and cyclogenesis latitude. The linear regression analysis produced a negative coefficient of -1.170 meaning that as the MEI increased from the mean, cyclogenesis longitude tended to decrease and vice versa.

Alterations in cyclogenesis longitude were also evident as the MEI fluctuated from the neutral phase. In the positive phase, clustering is more linear east to west across the western North Pacific basin than in the negative phase. The average longitude for cyclogenesis in the positive MEI phase was 143.52°E versus 133.69°E in the negative phase. Like the results of the

SOI mapped in Figure 4.3.2, far more tropical cyclones formed east of 140°E during El Niño-like conditions in Figure 4.3.3. In the positive phase of MEI, 55.8% of cyclogenesis occurred east of 140°E while only 23.3% met the same standard in the negative phase. The spatial analysis supports the positive correlation found between the MEI and longitude during the linear regression analysis. In general, as the MEI increases from the mean, tropical cyclogenesis longitude also increases (shifts east). Likewise, cyclogenesis cluster density increases near the Asian mainland during the negative MEI phase as cyclogenesis longitude tends to decrease (shift west).
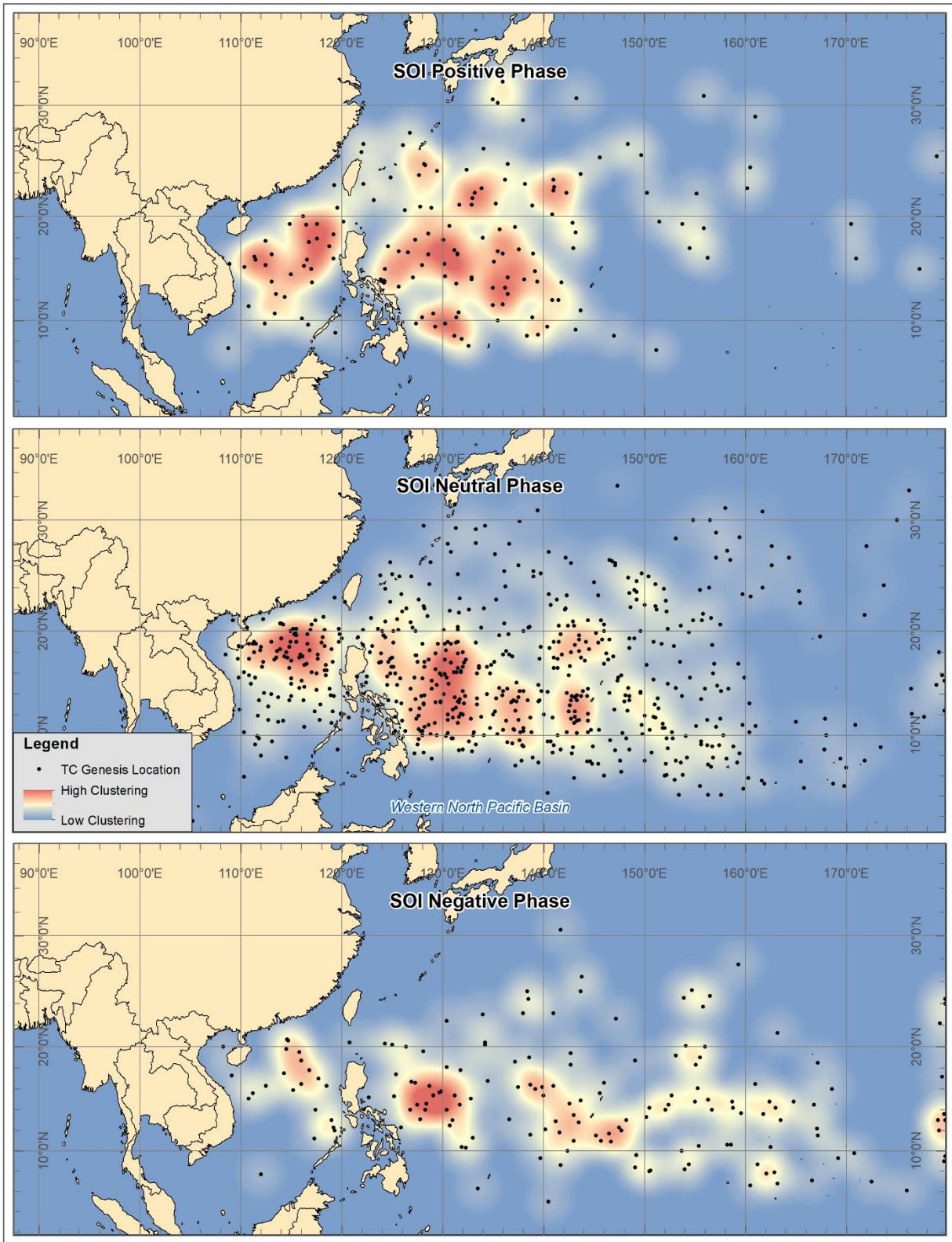
Figure 4.3.3. Point density maps for western North Pacific tropical cyclogenesis during positive, neutral, and negative phases of the MEI based on standard deviation from the mean.

Pacific Decadal Oscillation (PDO)

The PDO had the highest R^2 value (.042) of all the independent variables regressed against cyclogenesis latitude in the western North Pacific basin. The teleconnection index accounted for 4.2% of the variance in cyclogenesis latitude during the study period and 1.4% of the variance in longitude ($R^2 = .014$). Both regression analyses were found to be statistically significant at the 99% confidence interval ($p < .001$). Furthermore, the MEI revealed patterns of cyclogenesis cluster shifting in the western North Pacific basin during each phase of the teleconnection. The spatial analysis results are depicted in Figure 4.3.4.

During the positive PDO phase (0.855 to 2.41), tropical cyclogenesis tended to cluster between 8°N and 19°N latitude. Overall, 89% of cyclogenesis in the positive PDO phase occurred below 20°N latitude with an average latitude of 13.77°N. Adversely, only 64% of cyclogenesis occurred below 20°N latitude in the negative PDO phase (-1.454 to -3.05). The average latitude during the negative phase increased to 17.62°N. The spatial analysis results supported the negative correlation found between the MEI and tropical cyclogenesis. General trends found that as the MEI increases (decreases) from the mean, tropical cyclogenesis latitude decreases (increases).

Although the PDO only explained 1.4% of the variance in cyclogenesis longitude during the study period, some spatial trends were found that support the linear regression results. The positive correlation found between the MEI and cyclogenesis longitude can be examined in Figure 4.3.4. During the positive phase, the average longitude of cyclogenesis increased to 140.4°E over the mean value of 137.5°E. In the negative phase, cyclogenesis retracts toward the Asian mainland and clusters heavily near the eastern coast of the Philippines. The average latitude of cyclogenesis during the negative phase was 135.2°E.
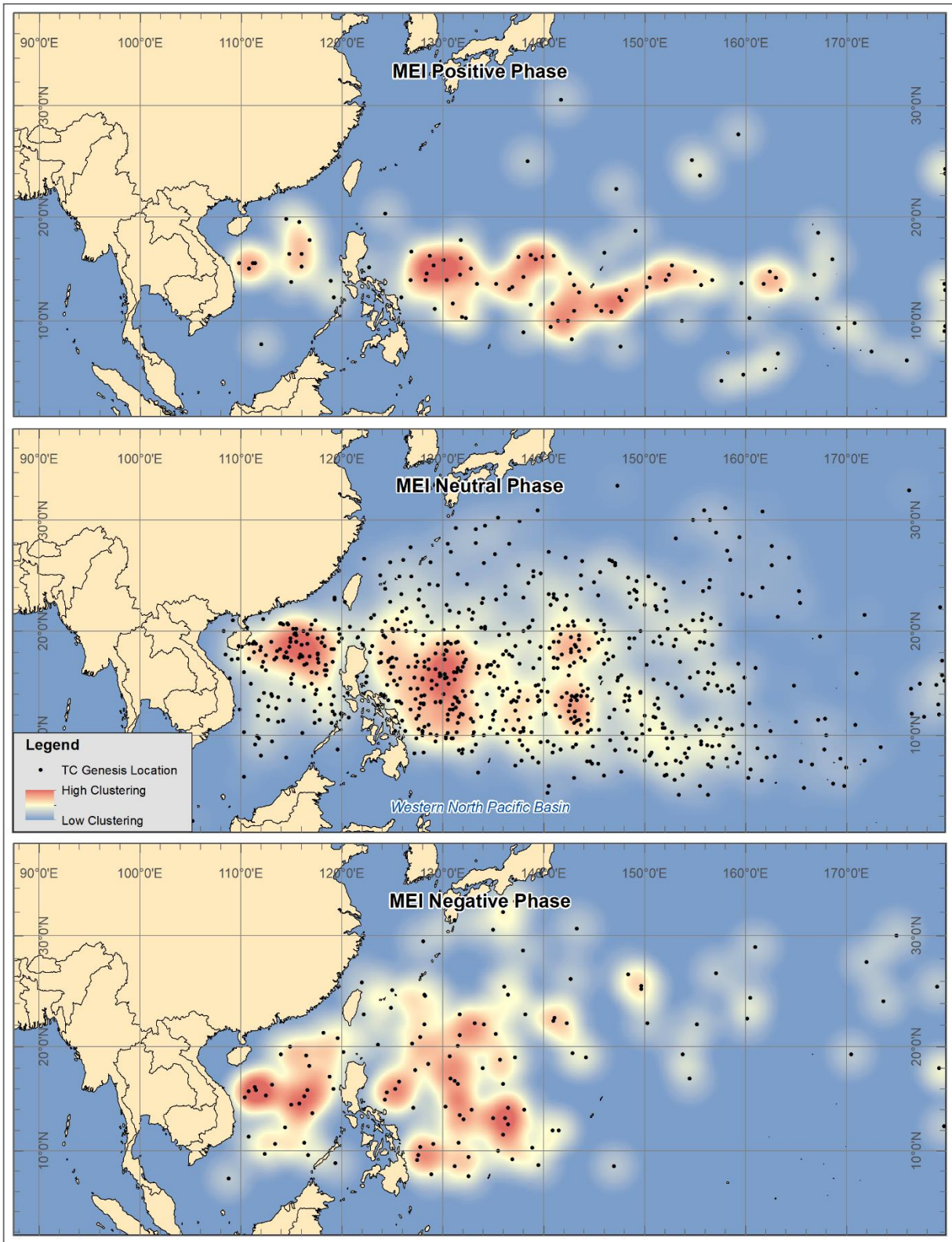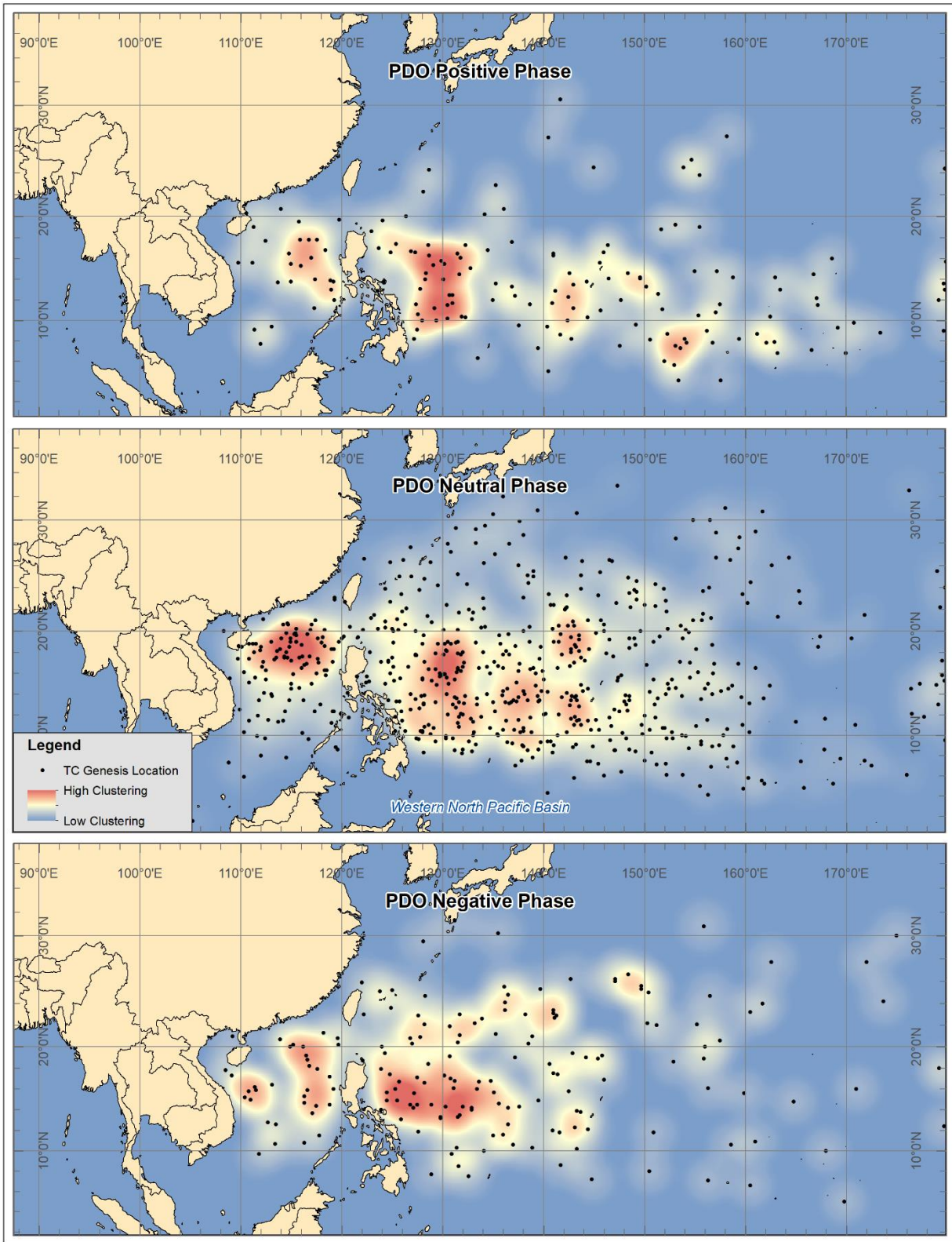
Figure 4.3.4. Point density maps for western North Pacific tropical cyclogenesis during positive, neutral, and negative phases of the PDO based on standard deviation from the mean.

Madden-Julian Oscillation (MJO)

Both the phase and amplitude of the MJO were regressed against the latitude/longitude

coordinates of western North Pacific tropical cyclogenesis for the study period 1979-2016. Each

parameter explained a statistically significant portion of the variance in cyclogenesis longitude at

the 99% confidence interval ($p < .001$) with R^2 values of .019 and .007, respectively. However,

neither the MJO phase nor the MJO amplitude were able to explain a statistically significant

portion of the variance in cyclogenesis longitude. Figures 4.3.5 and 4.3.6 display the results of

the MJO phase cluster density analysis using ESRI ArcGIS and the kernel density method.

Unlike the other teleconnection patterns, the MJO phase was mapped by each of the eight phases

instead of a positive, neutral, and negative classification based on the mean.

Table 4.3.3 contains information on the average latitude and the total number of tropical

cyclones occurring in each phase of the MJO. Phases 1 and 2 have the highest average latitude

values at 17.12°N and 17.5°N, respectively, with an average latitude between 16.74°N (phase 3)

to 14.95°N (phase 6) in the following six phases. These findings correspond with the negative

correlation found between the MJO phase and cyclogenesis latitude. Like the results found in the

eastern North Pacific Ocean, certain phases of the MJO had more activity than others. In the

western North Pacific, phase 6 was the most active with 166 storms reaching at least tropical

storm status. The heightened activity directly corresponds with the location of the MJO core over

the western Pacific in phases 6 and 7 and the increased convection that enhances tropical

cyclogenesis (see Figure 2.5).

MJO Phase	1	2	3	4	5	6	7	8
Avg. Lat. °N	17.12	17.5	16.74	15.66	16.52	14.95	15.4	15.08
Num. TCs	135	99	92	119	133	166	125	95

Table 4.3.3. MJO phase, average cyclogenesis latitude, and number of tropical cyclones
reaching at least tropical storm strength in the western North Pacific.
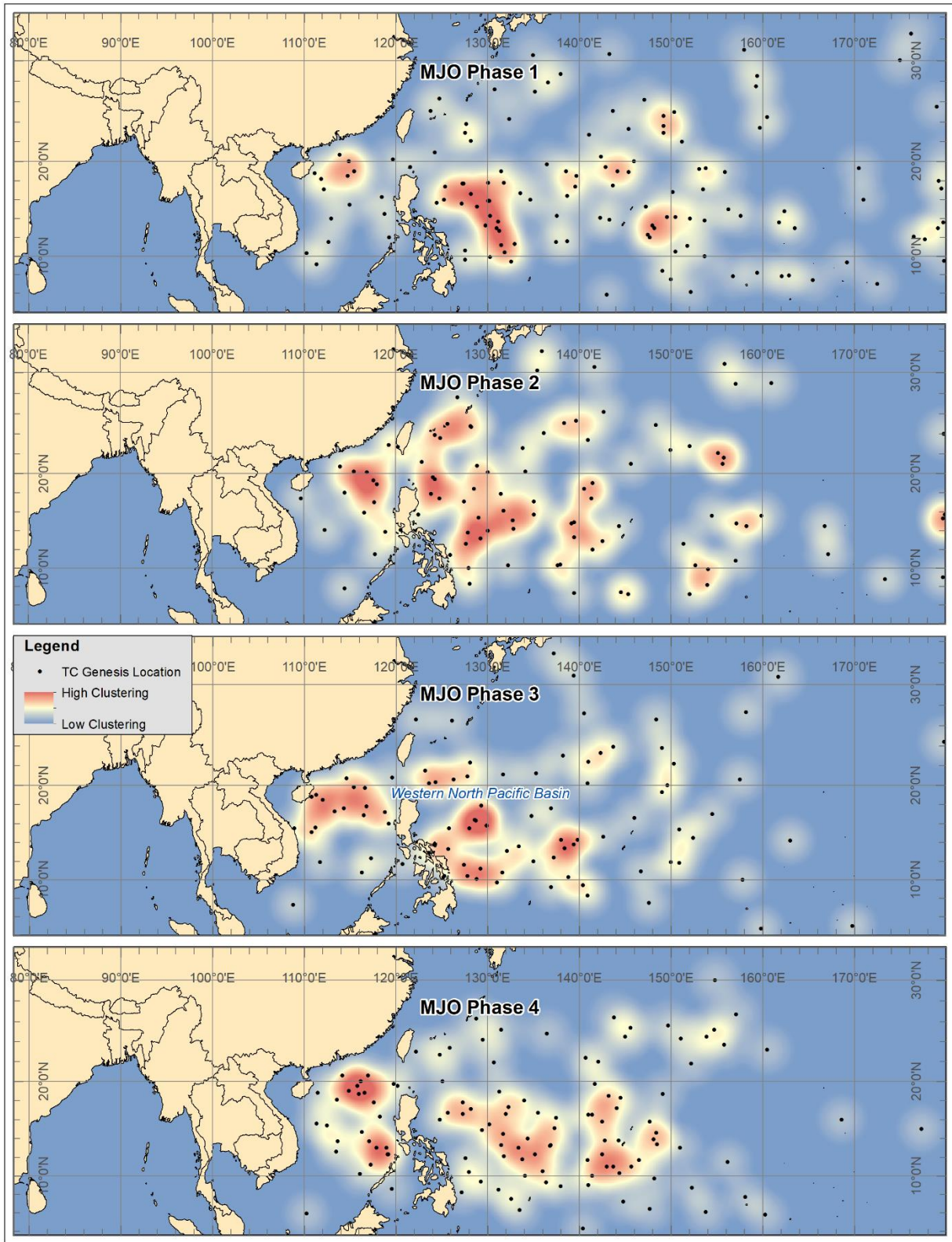
Figure 4.3.5. Point density maps for western North Pacific tropical cyclogenesis during phases 1-4 of the MJO.
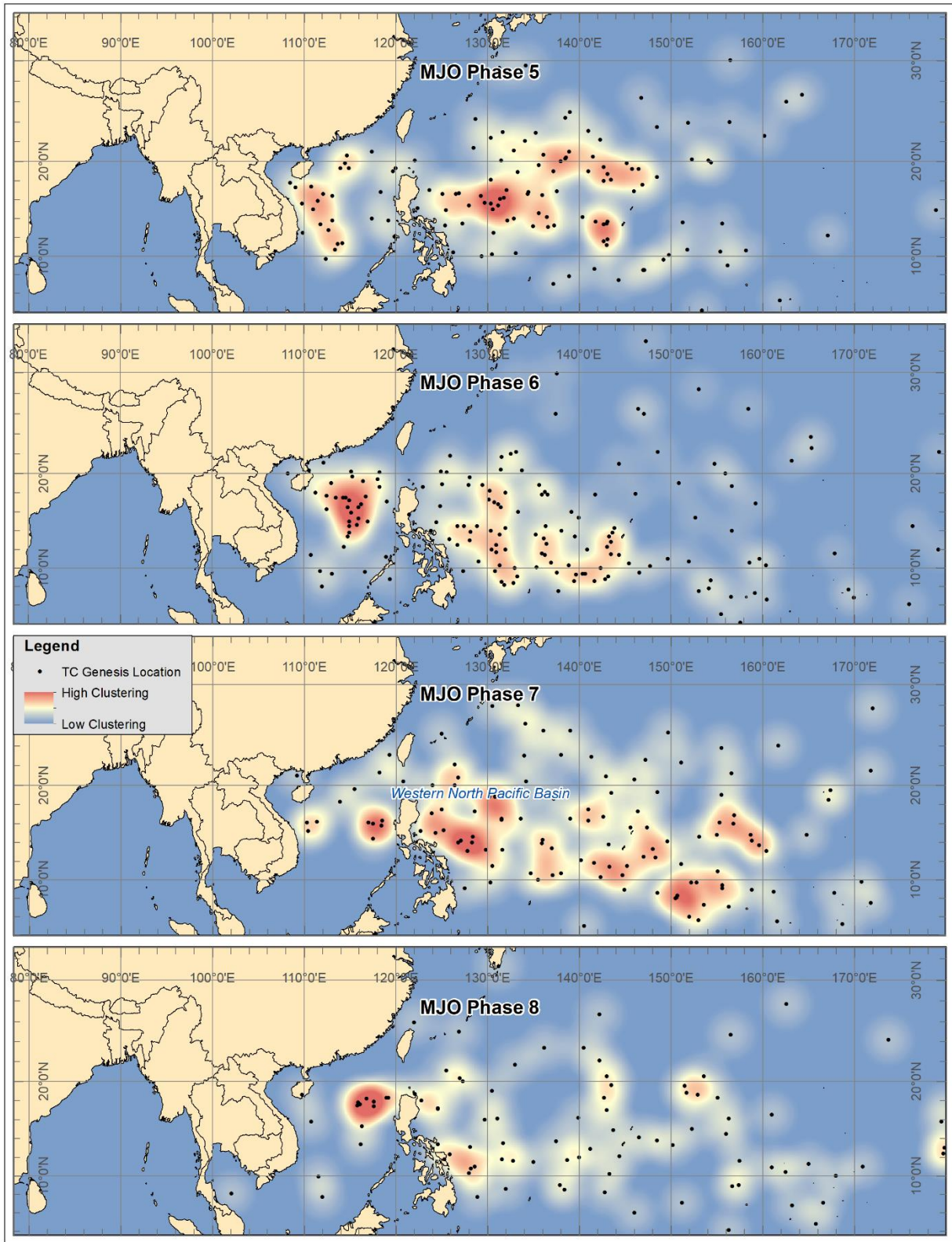
Figure 4.3.6. Point density maps for western North Pacific tropical cyclogenesis during phases 5-8 of the MJO.

61

Like the MJO phase, a negative correlation was also found between MJO amplitude and cyclogenesis latitude. Figure 4.3.7 visually depicts the results of the cluster density analysis for the MJO amplitude. The usual cyclogenesis hotspots are visible off the eastern coast of the Philippines and in the East China Sea during the neutral phase (1.793 to 0.577) with an average cyclogenesis latitude of 16.06°N. However, As the MJO amplitude deviated from the mean (1.185), the average latitude decreased to 14.81°N in the positive phase (1.794 to 3.328). Furthermore, the average latitude increased slightly from the mean to 16.08°N in the negative phase (0.576 to 4.47E-02) as the MEI amplitude value decreased.

Although the MJO amplitude did not provide statistically significant results for correlation with cyclogenesis longitude, some variation is evident throughout each of the three phases. The spatial trend tended to follow more of a positive correlation pattern where longitude increased and decreased with MJO amplitude. In the neutral phase, the average value for cyclogenesis longitude was 137.5°E. During the positive phase, this value increased to 138.43°E and decreased in the negative phase to 135.34°E.

Figure 4.3.7. Point density maps for western North Pacific tropical cyclogenesis during positive, neutral, and negative phases of MJO amplitude based on standard deviation from the mean.

Quasi-Biennial Oscillation (QBO)

Like the results in the eastern North Pacific Basin, the QBO only explained a marginal amount of the variance in tropical cyclogenesis latitude in the western Pacific Basin for the 964 measured storms. Similarly, the QBO did not produce statistically significant results for association with variance in cyclogenesis longitude for the study period. According to the linear regression analysis, the QBO explained less than 1% of the variance in latitude ($R^2 = .006$) with a p-value of .013.

The spatial analysis results (Figure 4.3.8) reveal similar patterns of clustering in the neutral (-18.740 to 9.476) and positive (9.477 to 15.620) phases of the QBO. Both phases feature dense clusters of cyclogenesis bordering the eastern coastline of the Philippines and in the East China Sea. During the positive QBO phase, the average latitude of cyclogenesis increased from the mean (15.4°N) to 16.24°N. In the negative phase, the average latitude of cyclogenesis increases to 17.31°N and cyclogenesis clusters become much more evident above 20°N latitude in Figure 4.3.8. The spatial trend is not completely representative of the negative correlation found between the QBO and cyclogenesis latitude since latitude increased slightly as the QBO index increased. However, latitude increased during the negative QBO phase as well, making the results more synchronous. After all, the QBO only explained less than 1% of the variance in latitude.

The QBO was one of the poorest indicators of the six tested teleconnection indices at explaining variance in cyclogenesis longitude. The regression analysis R^2 value was well below .01 (1%) in both the eastern and western Pacific basins. The spatial analysis results in Figure 4.3.8 provided no comprehensive patterns of cyclogenesis cluster shifting as the QBO fluctuated throughout the index range.

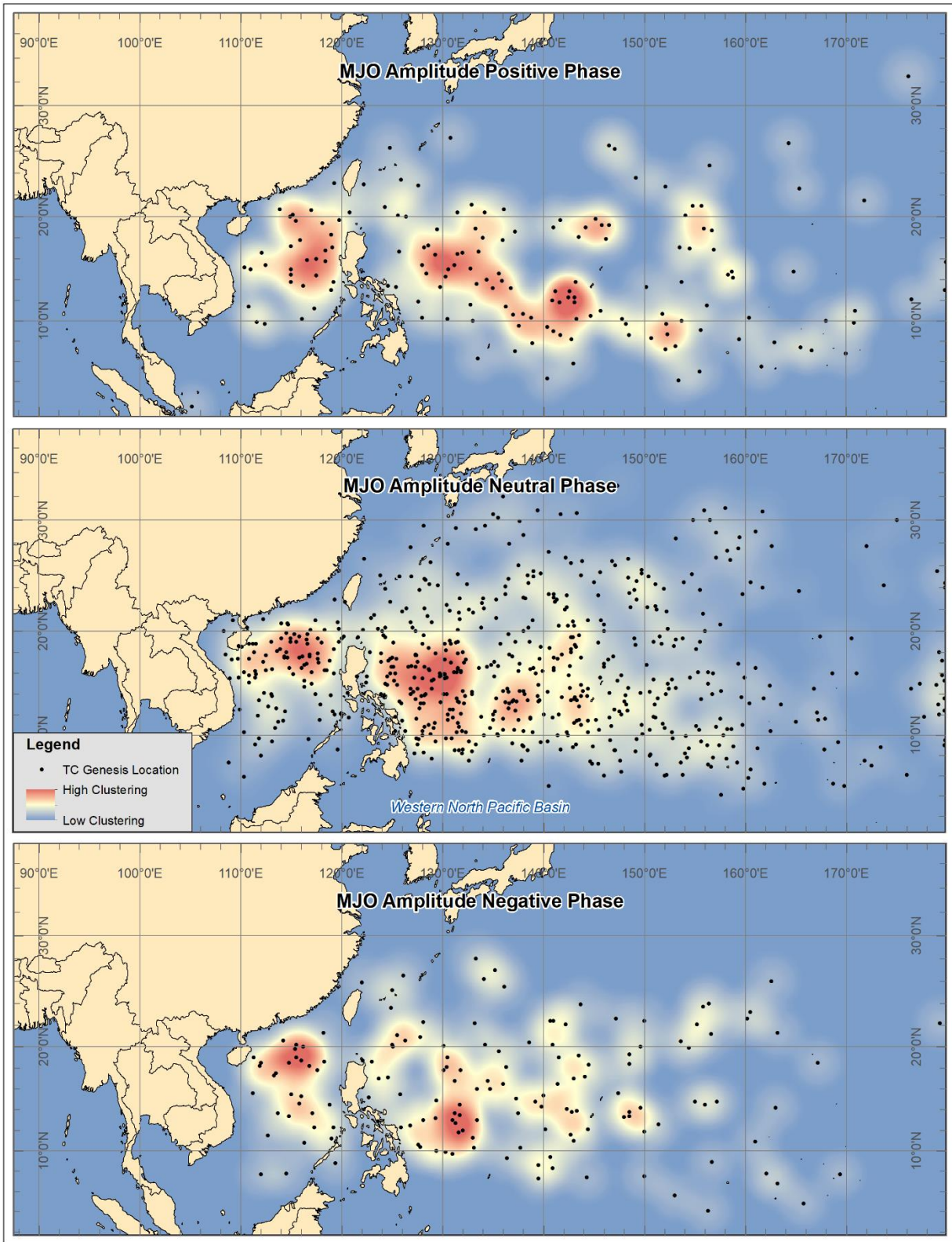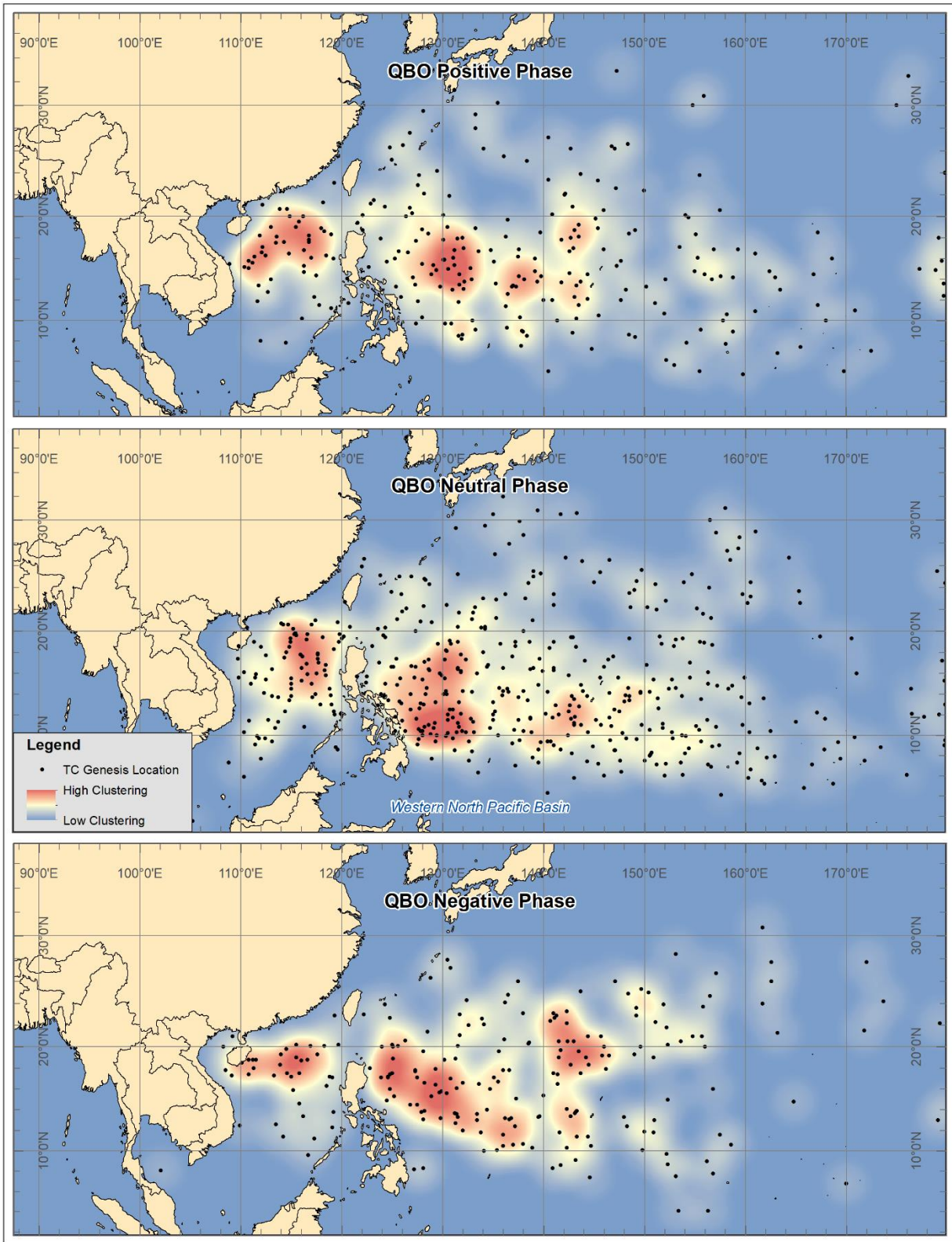**Figure 4.3.8.** Point density maps for western North Pacific tropical cyclogenesis during positive, neutral, and negative phases of the QBO based on standard deviation from the mean.

4.4 Western North Pacific Basin Combination Analysis

Like the eastern North Pacific combination analysis, the SOI, PDO, MJO phase, and QBO indices were also used for the western North Pacific multiple regression analysis. These four teleconnection indices had the most significant results from the simple linear regression independent testing and represented four independent teleconnection patterns. Sixteen combinations were created from a positive and negative phase of each index. Again, for the purposes of this study, MJO phase 1-4 was considered positive while 5-8 was considered negative. In total, 932 of the 964 storms were used for the multiple regression analysis; 32 storms were excluded for an index value equal to zero. Table 4.4.1 contains the results of the multiple linear regression analysis with a combination reference number, p-values, and R^2 values for both latitude and longitude analyses. The point density analysis maps are located in the appendix.

Combo #	SOI	PDO	MJO	QBO	Latitude p-value	Latitude R^2	Longitude p-value	Longitude R^2	Num. of Storms
1	+	-	+	-	0.020	0.131	0.024	0.126	87
2	-	+	-	+	0.157	0.108	0.481	0.058	62
3	+	+	-	-	0.844	0.025	0.354	0.076	60
4	-	-	+	+	0.049	0.213	0.183	0.144	44
5	+	-	-	-	0.015	0.153	0.679	0.031	78
6	-	+	+	+	0.012	0.227	0.220	0.108	54
7	+	-	-	+	0.655	0.044	0.190	0.107	58
8	-	+	+	-	0.335	0.086	0.137	0.128	55
9	+	+	+	-	0.159	0.113	0.573	0.052	59
10	-	-	-	+	0.005	0.194	0.045	0.130	74
11	+	+	-	+	0.880	0.103	0.125	0.485	15
12	-	-	+	-	0.048	0.192	0.344	0.095	49
13	+	-	+	+	0.212	0.094	0.425	0.063	63
14	-	+	-	-	0.690	0.033	0.263	0.075	71
15	+	+	+	+	0.359	0.216	0.609	0.140	22
16	-	-	-	-	0.261	0.066	0.458	0.046	81

Table 4.4.1. Results of the western North Pacific teleconnection combination analysis. Values in black were found to be statistically significant at the 95% confidence interval.

The western North Pacific teleconnection combination analysis produced more significant results than those of the eastern North Pacific. The relationship found between the independent variables and both latitude and longitude were somewhat more favorable. For the latitude regression analysis, five of the sixteen combinations produced statistically significant results at the 95% confidence interval and one combination produced a p-value at the 99% confidence interval ($p < .01$). For longitude, two combinations produced statistically significant results at the 95% threshold and explained 13% of the variance in longitude at best.

Combinations 1, 4, 5, 6, 10, and 12 had a significant relationship with latitude for the study period 1979-2016. Combination 6 (SOI - PDO + MJO + QBO +) explained the most significant portion of the variance in latitude (22.7%) for the 54 tropical cyclones that occurred during the conditions ($p = .012$; $R^2 = .227$). The inverse of combination 6 is combination 5 (SOI + PDO - MJO - QBO -). Combination 5 also had a statistically significant relationship with cyclogenesis latitude ($p = .015$) for the 78 tropical cyclones that occurred during the conditions and accounted for 15.3% of the variance ($R^2 = .153$). The cluster density analysis maps for combination 5 and 6 display some of the variance that occurred between the two combinations. During combination 5, cyclogenesis tended to occur at a higher latitude than during phase 6. Cyclogenesis also tended to occur more often west of 140°E during combination 5 and migrated east during combination 6.

Combinations 1 and 10 were the only two combinations to have a significant relationship with both latitude and longitude in the western North Pacific basin. Combination 1 (SOI + PDO - MJO + QBO -) had the highest amount of tropical cyclone activity for the study period with 87 storms reaching at least tropical storm strength. The multiple regression analysis accounted for 13.1% of the variance in latitude ($p = .02$; $R^2 = .131$) for the 87 storms and 12.6% of the variance

67

in longitude (p = .024; R^2 = .126). An examination of the cluster density maps reveals a drastic change in tropical cyclone geography between combination 1 and the inverse combination 2 (SOI - PDO + MJO - QBO +). During the conditions of combination 1, cyclogenesis was more frequent (25 more storms) and averaged a higher latitude than during combination 2. The average figure for combination 1 was 18.99°N versus 14.24°N during the inverse conditions in combination 2.

An above average number of tropical cyclones meeting the defined threshold also occurred during combination 10 (SOI - PDO - MJO - QBO +). The multiple regression analyses for both latitude and longitude revealed a statistically significant relationship with the combination parameters. For latitude, combination 10 explained 19.4% of the variance (p = .005; R^2 = .194) and 13% of the variance in longitude (p = .045; R^2 = .13) for the 74 storms occurring during the conditions. The cluster density maps for combination 10 and the inverse conditions (combination 9) are located in the appendix. Overall, tropical cyclogenesis tended to form further south and east during combination 10 than during combination 9. The average latitude decreased from 15.96°N to 14.34°N during the inverse while the average longitude increased from 135.02°E to 141.05°E during the conditions of combination 10.

CHAPTER 5
DISCUSSION

Both the simple (independent) and multiple (combination) regression analyses were successful at identifying the relationship between the teleconnection indices and the two dependent variables latitude and longitude. Each of the independent variables had a unique relationship with the geography of Pacific tropical cyclogenesis that was uncovered using statistical and spatial analysis. The purpose of this section is to further explain some of the individual characteristics of the teleconnection patterns and provide some possible reasoning for the way that they interacted with tropical cyclogenesis latitude/longitude during the study.

5.1 Eastern North Pacific Basin Independent Analysis

Pacific North American (PNA)

The PNA teleconnection pattern is the only independent variable that did not explain a significant portion of the variance in tropical cyclogenesis during the study period in the eastern North Pacific basin. A possible explanation for this lack of relationship with eastern North Pacific cyclogenesis geography is that the PNA acts as more of a steering mechanism for tropical cyclones after formation rather than a mechanism that inhibits growth or determines cyclogenesis location. The PNA has a large influence in the mid-latitudes and over the North American mainland in terms of weather and climate as it influences the flow of the jet stream over the continent (Wallace and Gutzler 1981). In the eastern North Pacific, most hurricanes occur below 20°N latitude where the PNA teleconnection does not have much influence. It is expected that the PNA has a greater influence on tropical cyclones that form or track into the midlatitudes rather than in the tropics. If the entire track of tropical cyclones was taken into consideration

during this study, perhaps the PNA teleconnection would have had a stronger correlation with the two dependent variables latitude and longitude.

El Niño Southern Oscillation (ENSO; SOI and MEI Indices)

In the eastern North Pacific, the ENSO pattern was found to have a significant impact on the geography of tropical cyclogenesis using both the SOI and MEI indices. The drastic changes in latitude and longitude during the positive versus the negative phase of both indices can be explained by the very nature of the ENSO and the recipe that tropical cyclones need for formation and growth. During the positive phase of SOI (negative phase of MEI), the ENSO is in the La Niña phase where ocean water is colder than normal off the coast of Peru. The cooler water impacts the strength and location of tropical cyclones in the eastern North Pacific since one of the key ingredients of tropical cyclone formation is an abundance of warm water above 79°F (26°C). The cold-water upwelling off the coast of Peru during La Niña inhibits tropical cyclone growth; therefore, only storms that form further north in the eastern North Pacific develop into tropical storms and major tropical cyclones during the positive SOI phase. Likewise, in the negative phase of SOI (positive phase of MEI), there is a larger than normal pool of warm water off the coast of Peru that extends westward. The amplified area of warm water in the eastern North Pacific turns into a breeding ground for tropical cyclones and details the large shift in cyclogenesis toward the equator during El Niño conditions (McPhaden 2002; Hanley et al. 2003).

Pacific Decadal Oscillation (PDO)

The PDO is a long-term teleconnection pattern that is normally dominated by a persistent phase for multiple decades. According to Mantua et al. (1997), cool (negative) PDO patterns were prevalent from 1890-1924 and from 1947-1976. Warm (positive) patterns dominated from

70

1925-1946 and from 1977 to the mid-1990's. For the study period 1979-2016, the results largely corresponded with the findings by Mantua et al. (1997). The period 1979 to the mid-1990s was predominantly positive with some small fluctuation. Likewise, the late 1990s and 2000s fell largely in the negative phase with some neutrality.

The negative correlation between the PDO and cyclogenesis latitude is largely a response to SST variation in the eastern North Pacific. During the positive PDO phase, tropical cyclones tended to cluster at lower latitudes as a result of the increased SSTs in the eastern and central North Pacific. The increased midlatitude westerly wind flow during the positive PDO phase could also have an effect on tropical cyclogenesis by introducing wind shear that inhibits growth. In the negative phase, a dramatic shift in tropical cyclogenesis can also be attributed largely to SST variation. During this phase, a pool of cooler than normal SSTs occurs in the central Pacific near the equator with average or slightly above average SSTs near the coast of Central and South America. The SST anomaly is likely one of the driving forces behind the northeasterly shift in tropical cyclogenesis during the negative phase of the PDO. However, the PDO only accounted for roughly 3% of the variance in cyclogenesis latitude so there are a multitude of factors that determine cyclogenesis geography.

Madden-Julian Oscillation (MJO)

Although the MJO phase and amplitude parameters were both used in this study, only the MJO phase had a statistically significant correlation with latitude and longitude of tropical cyclogenesis in the eastern North Pacific. However, the MJO phase only explained approximately 1% of the variance in cyclogenesis latitude and longitude, providing a weak correlation between the variables. Since MJO phase only explains roughly 1% of the variance in tropical cyclogenesis latitude and longitude in the eastern North Pacific basin, perhaps the more

important aspect to stress with the MJO is how it influences overall tropical cyclone activity. It is known that the MJO has a direct influence on tropical cyclogenesis, but this study further solidifies results found in previous studies and gives them a spatial component (Maloney and Hartman 2000). In addition to patterns in cyclogenesis clustering, it was found that tropical cyclones were 1.8 times more likely to form in MJO phase 8, 1, and 2 than in phase 3-7 in the eastern North Pacific basin for the specified study period.

Quasi-Biennial Oscillation (QBO)

The QBO teleconnection was found to have a statistically significant correlation with tropical cyclogenesis latitude but not longitude for the study period 1979-2016. Like the MJO, however, the QBO explained less than 1% of the variance in cyclogenesis latitude for the 626 tropical cyclones tested in the eastern North Pacific basin and had a weak correlation. The weak correlation is likely due to the fact that the QBO is an alteration of wind patterns at very high altitudes in the stratosphere and upper troposphere. Most of the key atmospheric components that are necessary for cyclogenesis to occur are found in the troposphere below the height at which the QBO occurs. As mentioned in Chapter 2, the QBO has been found to have an influence on tropical cyclone track and intensity in previous studies (Angell et al. 1969; Ho et al. 2009), but only has a weak influence on tropical cyclogenesis latitude in the eastern North Pacific.

5.2 Eastern North Pacific Basin Combination Analysis

The teleconnection combination analysis method was used to test every possible combination of the four most statistically significant explanatory variables in the independent analysis (SOI, PDO, MJO, QBO). Overall, the combinations were not efficient at explaining variance in tropical cyclogenesis latitude or longitude during the study period. For the

combinations that provided a statistically significant relationship with cyclogenesis latitude or longitude, it was not abnormal for only one of the four variables to have a significant relationship.

The cluster density maps in the appendix are sporadic and show very few highlights in cluster shifting among any of the sixteen combinations. On the other hand, the combinations do provide insight into the way that different teleconnection combinations affect cyclogenesis in the eastern North Pacific basin. In many cases, there are drastic differences in the number of tropical cyclones that occur during one combination and the inverse. Combination 1, for example, produced 56 tropical cyclones reaching at least tropical storm strength during the study period while the inverse (combination 2) produced only 26 tropical cyclones meeting the same threshold. As expected, combinations where warmer than normal SSTs are found in the eastern North Pacific were generally more productive of tropical cyclones. Combination 6 (SOI -, PDO +, MJO +, QBO +), for example, is composed of El Niño-like conditions (negative SOI) with a warm (positive) PDO and produced the second highest number of tropical cyclones (53). The MJO also seemed to greatly influence the number of tropical cyclones that occurred during each combination. Above average tropical cyclone frequency was more likely during the positive MJO phase when convection was strongest over the eastern North Pacific region.

5.3 Western North Pacific Basin Independent Analysis

West Pacific (WP)

The WP teleconnection pattern is the only explanatory variable tested in the western North Pacific basin that did not explain a significant portion of the variance in cyclogenesis latitude or longitude. Like the PNA teleconnection tested in the eastern North Pacific, the WP

measures fluctuations in geopotential height in the atmosphere and has been proven to effect tropical cyclone track, intensity and frequency in the western North Pacific (Choi and Moon 2012). However, Choi and Moon (2012) only used eight of the most positive and negative years of the WP teleconnection in their study where this research uses a much longer timespan of 37 consecutive years. By using a similar methodology as Choi and Moon and isolating strong positive and negative WP teleconnection events, it is possible that more significant results could be found for correlation with tropical cyclogenesis geography.

El Niño Southern Oscillation (ENSO; SOI and MEI Indices)

The ENSO teleconnection pattern accounted for the highest explanation of variance in tropical cyclogenesis latitude and longitude using the SOI and MEI indices than any other variable used in this research. The findings further reinforce the fact that the ENSO teleconnection is one of the most influential patterns of natural climatic variability. The results of this research strongly coincide with those of Chia and Ropelewski (2002) who used a similar methodology to study tropical cyclogenesis geography in relation to ENSO from 1979-1999. However, the study period for this analysis was extended from 20 to 37 years (1979-2016) but the results remained largely the same. In La Niña conditions, tropical cyclones tended to shift northwest of the mean cyclogenesis location; likewise, they tended to shift southeast during El Niño conditions. Although the SOI and MEI indices were both significant determinant variables, neither of the indices could explain greater than 10% of the variance in tropical cyclogenesis. In order to account for a greater portion of the variance, many other factors like wind shear, SST, and other teleconnection pattern phases would have to be considered.

Pacific Decadal Oscillation (PDO)

The pattern of cyclogenesis clustering during the positive and negative phases of the PDO largely follows the SST anomaly patterns. In the positive phase, SSTs are colder than normal in the North Pacific, with average to slightly below average temperatures in the western North Pacific. The cool SST anomaly keeps cyclogenesis mainly below 20°N latitude during the positive phase. In the negative PDO phase, however, the SSTs in the north and western Pacific are above average and are more favorable for cyclogenesis above 20°N. The PDO also had a small effect on the longitude of tropical cyclogenesis during the study period; however, the teleconnection only explained 1.4% of the variance. The PDO had a stronger correlation with western North Pacific latitude and explained 4.2% of the variance for the same study period.

Madden-Julian Oscillation (MJO)

Unlike the eastern North Pacific basin, both the MJO phase and amplitude produced statistically significant results for correlation with cyclogenesis latitude. However, neither parameter could explain more than 2% of the variance in cyclogenesis latitude proving that the correlation is weak. Both the MJO amplitude and phase had a negative correlation with latitude during the study period. The results provide insight for forecasting that as the MJO phase or amplitude increase, tropical cyclogenesis is more likely to occur at a lower latitude than normal; this is especially true whenever the MJO is over the western North Pacific quadrant in phases 6 and 7 with a strong positive amplitude. ENSO can also affect patterns of the MJO by increasing (decreasing) the speed at which the MJO propagates eastward during El Niño (La Niña) conditions and altering normal wind patterns over the western North Pacific (Pohl and Matthews 2007). Teleconnection relationships like the one between the ENSO and the MJO further

reinforce the reasoning for studying combination patterns and their effects on tropical cyclogenesis.

Quasi-Biennial Oscillation (QBO)

The eastern and western North Pacific basins had a similar relationship with the QBO teleconnection. Both had a weak correlation with changes in cyclogenesis latitude related to the QBO teleconnection and a non-significant association with cyclogenesis longitude. Overall, this study found that the QBO is not an efficient predictor of tropical cyclogenesis geography. Although the QBO has been found to have a significant effect on the track of tropical cyclones in the western North Pacific (Ho et al. 2009), the teleconnection has a minimal influence on cyclogenesis geography.

5.4 Western North Pacific Basin Combination Analysis

The multiple linear regression and spatial analysis for the teleconnection combinations in the western North Pacific produced quality results that accentuate the volatility of certain phase combinations and variations in cyclogenesis geography. Like the eastern North Pacific, though, the four explanatory variables did not seem to accumulatively account for variation in cyclogenesis latitude or longitude. There were always one or two variables that had a significant correlation with the dependent variables and the others were non-significant.

Again, like the eastern North Pacific analysis, the western North Pacific combination analysis provided very useful information on not only the geographic variability in cyclogenesis but also frequency. Tropical cyclone frequency varied greatly from 15 (combination 11) to 87 (combination 1) storms occurring under each combination in the 1979-2016 study period. Tropical cyclone frequency tended to be above average whenever the PDO and/or the MJO were

in the negative phase; this corresponds with warmer than normal water in the western North Pacific during the negative PDO phase and enhanced convection in the basin during the MJO negative phase.

In future studies, a more efficient combination analysis might produce more significant results. For example, using a methodology like that of Choi and Moon (2012) where high positive or low negative index values are examined that represent strong phases of the teleconnection pattern might uncover a more distinct pattern of the teleconnection impact on cyclogenesis might by eliminating the neutral cases. Another method of study could examine just two teleconnections at a time. For example, a researcher could study the influence of the PDO and the ENSO simultaneously in all possible combinations since they are well known to influence tropical cyclone activity in the North Pacific basin (Mantua et al. 1997).

CHAPTER 6
CONCLUSION

The findings of this study indicate that many of the teleconnection patterns found in the Northern Hemisphere do, in fact, have an influence on the geography of Pacific tropical cyclone genesis. Four of the six teleconnection patterns used in this research (ENSO, PDO, MJO, and QBO) were found to have a statistically significant relationship with variations in cyclogenesis latitude and/or longitude at the 95% confidence interval or greater. The PNA and WP teleconnection patterns were not found to have a significant influence on tropical cyclogenesis geography in their respective areas of dominance during the study period 1979-2016.

In the eastern North Pacific, the SOI and MEI indices (representative of ENSO) had the strongest relationship with cyclogenesis latitude and longitude for the 626 tropical cyclones occurring during the study period. The relationship is not surprising since ENSO has been linked to drastic changes in cyclogenesis frequency and intensity in prior studies. Although the SOI only explained 4.9% of the variance in cyclogenesis latitude at best, the spatial analysis cluster density maps show drastic shifts in clustering during the positive, neutral, and negative phases. For each of the teleconnection patterns, the cluster density maps provide excellent visual representation of the statistical analysis results.

In the western North Pacific, the independent teleconnection analyses performed similarly to the eastern North Pacific basin. The WP teleconnection pattern was not found to have a significant relationship with cyclogenesis latitude or longitude during the study period. Again, the ENSO indices (SOI and MEI) performed well during analysis but the PDO explained a greater portion of the variance in cyclogenesis latitude for the 964 tropical cyclones tested in the western North Pacific basin. Interestingly, the independent teleconnections had a stronger

78

relationship with cyclogenesis longitude in the western North Pacific basin than in the eastern North Pacific. The SOI and MEI indices explained 4.6% and 3.6% of the variance in longitude, respectively.

The teleconnection combination analysis in both basins provided some statistically significant results but were largely non-significant for the study period. In the eastern North Pacific basin, the multiple linear regression analyses were inefficient at identifying the relationship between the explanatory variables and the dependent variables. Although the western North Pacific basin results were more favorable, many of the teleconnection combinations still produced non-significant or marginal results that showed a weak correlation between the variables. The combination analysis provided more indicative results for tropical cyclogenesis frequency rather than tropical cyclone geography. In many cases, there were drastic changes in tropical cyclone frequency and geography between a combination pattern and the inverse pattern. Some of these combinations were expected to produce above average tropical cyclone frequencies while others were more surprising.

Overall, the independent variables tended to explain more of the variance in latitude than longitude in both study areas. Although the independent variables explained a relatively small portion of the variance in cyclogenesis latitude and/or longitude, the data used in this study provide useful insight into the influence that teleconnections have on tropical cyclogenesis. The formation of tropical cyclones is one of the most complex mechanisms of atmospheric science study, and this research has furthered the body of knowledge toward their understanding. By testing the variables independently and in combination, this exhaustive study has analyzed a great amount of data to provide quality results toward the better understanding of tropical cyclogenesis geography.

BIBLIOGRAPHY

Angell, J. K., Korshover, J., and Cotten, G.F. (1969). Quasi-Biennial Variations in the "Centers of Action." *Monthly Weather Review*, 97(12), 867-872.

Australian Bureau of Meteorology. (2017). *Madden-Julian Oscillation (MJO)*, concatenated, 1979-2016 [Data File]. Retrieved from http://www.bom.gov.au/climate/mjo/.

Baldwin, M.P., Gray, L.J., Dunkerton, T.J., Hamilton, K., Haynes, P.H., Randel, W.J., Holton, J.R., Alexander, M.J., Hirota, I., Horinouchi, T., Jones, D.B.A., Kinnersley, J.S., Marquardt, C., Sato, K., and Takahaski, M. (2001). The Quasi-Biennial Oscillation. *Reviews of Geophysics*, 39(2), 179-229.

Camargo, S.J., and Sobel, A.H. (2005). Western North Pacific Tropical Cyclone Intensity and ENSO. *Journal of Climate*, 18, 2996-3006.

Camargo, S.J., Emanuel, K.A., and Sobel, A.H. (2007). Use of a Genesis Potential Index to Diagnose ENSO Effects on Tropical Cyclone Genesis. *Journal of Climate*, 20, 4819-4834.

Chia, H.H., and Ropelewski, C.F. (2002). The Interannual Variability in the Genesis Location of Tropical Cyclones in the Northwest Pacific. *Journal of Climate*, 15, 2934-2944.

Choi, K., and Moon, L. (2012). Influence of the Western Pacific Teleconnection Pattern on Western North Pacific Tropical Cyclone Activity. *Dynamics of Atmospheres and Oceans*, 57, 1-16.

Emanuel, K.A. (1987). The Dependence of Hurricane Intensity on Climate. *Nature*, 326(6112), 483-485.

ENSO and PDO Models. Retrieved from http://www.intellicast.com/Community/Content.aspx?ref=rss&a=151

Gottschalck, J., Kousky, V., Higgins, W., and L'Heureux, M. (n.d.). Madden Julian Oscillation (MJO). Retrieved from http://www.cpc.noaa.gov/products/precip/CWlink/MJO/MJO_summary.pdf.

Gray, W.M. (1975). Tropical Cyclone Genesis. Dept. of Atmos. Sci. Paper No. 234, Colo. State Univ., Ft. Collins, CO, 121 pp.

Gray, W.M. (1979). "Hurricanes: Their formation, structure and likely role in the tropical circulation" Meteorology Over Tropical Oceans. D. B. Shaw (Ed.), Roy. Meteor. Soc., James Glaisher House, Grenville Place, Bracknell, Berkshire, RG12 1BX, 155-218.

Hanley, D.E., Bourassa, M.A., O'Brien, J.J., Smith, S.R., and Spade, E.R. (2003). A Quantitative Evaluation of ENSO Indices. *Journal of Climate*, 16, 1249-1258.

Hare, S. R. (1996). Low-frequency climate variability and salmon production. Ph.D. thesis, University of Washington, Seattle, 306 pp.

Higgins, R.W., and Shi, W. (2001). Intercomparison of the Principal Modes of Interannual and Intraseasonal Variability of the North American Monsoon System. *Journal of Climate*, 14, 403-417.

Ho, C.H., Kim, H.S., Jeong, J.H., and Son, S.W. (2009). Influence of Stratospheric Quasi-Biennial Oscillation on Tropical Cyclone Tracks in the Western North Pacific. *Geophysical Research Letters*, 36, L06702.

Japan Meteorological Agency Regional Specialized Meteorological Center Tokyo Typhoon Center. (2017). *RSMC Best Track Data*, concatenated, 1979-2016 [Data File]. Retrieved from http://www.jma.go.jp/jma/jma-eng/jma-center/rsmc-hp-pub-eg/trackarchives.html.

Klotzbach, P.J., and Gray, W.M. (2004). Updated 6-11 Month Prediction of Atlantic Basin Seasonal Hurricane Activity. *Weather and Forecasting*, 19, 917-934.

Linkin, M.E., and Nigam, S. (2008). The North Pacific Oscillation-West Pacific Teleconnection Pattern: Mature-Phase Structure and Winter Impacts. *Journal of Climate*, 21, 1979-1997.

Maloney, E.D., and Hartman, D.L. (2000). Modulation of Eastern North Pacific Hurricanes by the Madden–Julian Oscillation. *Journal of Climate*, 13, 1451-1460.

Maloney, E.D., and Hartman, D.L. (2001). The Madden–Julian Oscillation, Barotropic Dynamics, and North Pacific Tropical Cyclone Formation. Part I: Observations. *Journal Atmos. Sci.*, 58, 2545-2558.

Mantua, N.J. (2002). Pacific-Decadal Oscillation. *Encyclopedia of Global Environmental Change*, 592-594.

Mantua, N.J., Hare, S.R., Zhang, Y., Wallace, J.M., and Francis, R.C. (1997). A Pacific Interdecadal Climate Oscillation with Impacts on Salmon Production. *Bulletin of the American Meteorological Society*, 78(6), 1069-1079.

McPhaden, M.J. (2002). El Niño and La Niña: Causes and Global Consequences. *Encyclopedia of Global Environmental Change*, 1, 353-370.

MJO Phase-Space Diagram. Retrieved from http://la.climatologie.free.fr/MJO/MJO1-english.htm.

National Hurricane Center Data Archive. (2017). *Best Track Data (HURDAT2)*, concatenated, 1979-2016 [Data File]. Retrieved from https://www.nhc.noaa.gov/data/#hurdat.

National Oceanic and Atmospheric Administration Earth Systems Research Laboratory Physical Sciences Division. (2017). *Climate Indices: Monthly Atmospheric and Oceanic Time Series*, concatenated, 1979-2016 [Data Files]. Retrieved from https://www.esrl.noaa.gov/psd/data/climateindices/list/.

National Oceanic and Atmospheric Administration Hurricane Research Division. (n.d.). *Tropical Cyclone Climatology*. Retrieved From http://www.aoml.noaa.gov/hrd/tcfaq/E10.html.

National Oceanic and Atmospheric Administration National Centers for Environmental Information. (2017). *Pacific Decadal Oscillation (PDO),* concatenated, 1979-2016 [Data File]. Retrieved from https://www.ncdc.noaa.gov/teleconnections/pdo/.

North Carolina Climate Office. PNA Model. Retrieved from
	https://climate.ncsu.edu/climate/patterns/pna.

Oliver, A. (2010). El Niño Southern Oscillation, Climate Indices & their relationship with Wind
	Speed in the Texas Panhandle. RES Americas, Broomfield, CO.

Palmén, E. (1956). A review of Knowledge on the Formation and Development of Tropical
	Cyclones. *Proc. Of the Tropical Cyclone Symposium*, Bureau of Meteorology, Brisbane,
	Australia, 213-232.

Pohl, B., and Matthews, A.J. (2007). Observed Changes in the Lifetime and Amplitude of the
	Madden–Julian Oscillation Associated with Interannual ENSO Sea Surface Temperature
	Anomalies. *Journal of Climate*, 20, 2659-2674.

Ramage, C.S. (1959). Hurricane Development. *Journal of Meteorology*, 16, 227-237.

Reed, R.J., and Rogers, D.G. (1962). The Circulation of the Tropical Stratosphere in the Years
	1954-1960. *Journal Atmos. Sci.*, 19, 127-135.

Rohli, R. V., and Vega, A.J. (2012). *Climatology*. 2nd ed., Jones & Bartlett Learning.

Rui, H. and B. Wang (1990). Development characteristics and dynamic structure of tropical
	intraseasonal convection anomalies, *Journal Atmos. Sci.*, 47, 357-379.

Shimura, T., Mori, N., and Mase, H. (2013). Ocean Waves and Teleconnection Patterns in the
	Northern Hemisphere. *Journal of Climate*, 26, 8654-8670.

Silverman, B.W. (1986). Density Estimation of Statistics and Data Analysis. *Monographs on
	Statistics and Applied Probability*. Chapman & Hall, London – New York, 175 pp.
	Retrieved from https://ned.ipac.caltech.edu/level5/March02/Silverman/paper.pdf.

Stoner, A.M., Hayhoe, K., and Wuebbles, D.J. (2009). Assessing General Circulation Model
	Simulations of Atmospheric Teleconnection Patterns. *Journal of Climate*, 22, 4348-4372.

Walker, G. T. (1923). Correlation in seasonal variations of weather. VIII. A preliminary study of
	world-weather. *Mem. Indian Meteor. Dep*., 24 (Part 4), 75–131.

Wallace, J.M., and Gutzler, D.S. (1981). Teleconnections in the Geopotential Height Field
	during the Northern Hemisphere Winter. *Monthly Weather Review*, 109, 784-812.

Wang, H., Kumar, A., Wang, W., and Xue, Y. (2012). Influence of ENSO on Pacific Decadal
	Variability: An Analysis Based on the NCEP Climate Forecast System. *Journal of
	Climate,* 25, 6136-6151.

Wheeler, M.C., and Hendon, H.H. (2004). An All-Season Real-Time Multivariate MJO Index:
	Development of an Index for Monitoring and Prediction. *Monthly Weather Review*, 132,
	1917-1932.

Whitney, L.D., and Hobgood, J.S. (1997). The Relationship between Sea Surface Temperatures
	and Maximum Intensities of Tropical Cyclones in the Eastern North Pacific Ocean.
	Journal of Climate, 10, 2921-2930.

Wolter, K., and Timlin, M.S. (1993). Monitoring ENSO in COADS with a seasonally adjusted principal component index. *Proc. of the 17th Climate Diagnostics Workshop*, Norman, OK, NOAA/NMC/CAC, NSSL, Oklahoma Clim. Survey, CIMMS and the School of Meteor., Univ. of Oklahoma, 52-57.

Zhang, C. (2013). Madden-Julian Oscillation: Bridging Weather and Climate. *Bull. Amer. Meteor. Soc*., 94, 1849-1870.

Zhang, C., and Gottschalck, J. (2002). SST Anomolies of ENSO and the Madden-Julian Oscillation in the Equatorial Pacific. *Journal of Climate*, 15, 2429-2445.

APPENDIX A:
OFFICE OF RESEARCH INTEGRITY APPROVAL LETTER

MARSHALL UNIVERSITY®

www.marshall.edu

Office of Research Integrity

March 13, 2018

Nicholas Adkins
4009 Kanawha Tpke., Apt. 7H
South Charleston, WV 25309

Dear Mr. Adkins:

This letter is in response to the submitted thesis abstract entitled *"The Influence of Northern Hemisphere Teleconnections on the Geography of Pacific Tropical Cyclone Genesis."* After assessing the abstract, it has been deemed not to be human subject research and therefore exempt from oversight of the Marshall University Institutional Review Board (IRB). The Code of Federal Regulations (45CFR46) has set forth the criteria utilized in making this determination. Since the information in this study does not involve human subjects as defined in the above referenced instruction, it is not considered human subject research. If there are any changes to the abstract you provided then you would need to resubmit that information to the Office of Research Integrity for review and a determination.

I appreciate your willingness to submit the abstract for determination. Please feel free to contact the Office of Research Integrity if you have any questions regarding future protocols that may require IRB review.

Sincerely,

Bruce F. Day, ThD, CIP
Director

WE ARE... MARSHALL.

One John Marshall Drive • Huntington, West Virginia 25755 • Tel 304/696-4303
A State University of West Virginia • An Affirmative Action/Equal Opportunity Employer

APPENDIX B:
DATA DEFINITIONS

ENSO: El Niño Southern Oscillation

ESRI: Environmental Systems Research Institute

ESRL: Earth Systems Research Laboratory

GIS: Geographic Information System

MEI: Multivariate El Niño Southern Oscillation Index

MJO: Madden-Julian Oscillation

NCEI: National Centers for Environmental Information

NHC: National Hurricane Center

NOAA: National Oceanic and Atmospheric Administration

PDO: Pacific Decadal Oscillation

PNA: Pacific-North American

QBO: Quasi-Biennial Oscillation

RSMC: Regional Specialized Meteorological Center

SLP: Sea Level Pressure

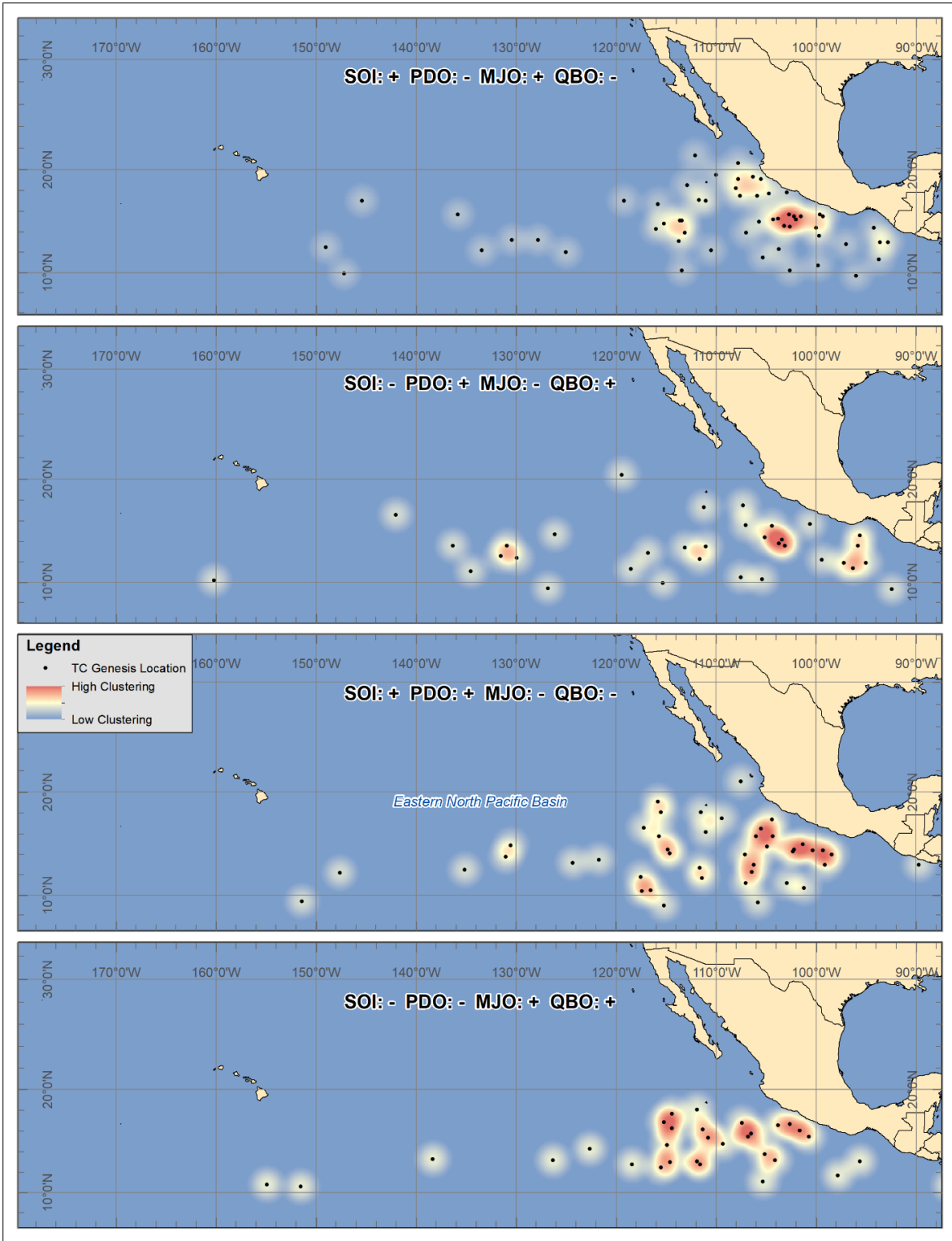**SO:** Southern Oscillation

SOI: Southern Oscillation Index

SST: Sea Surface Temperature

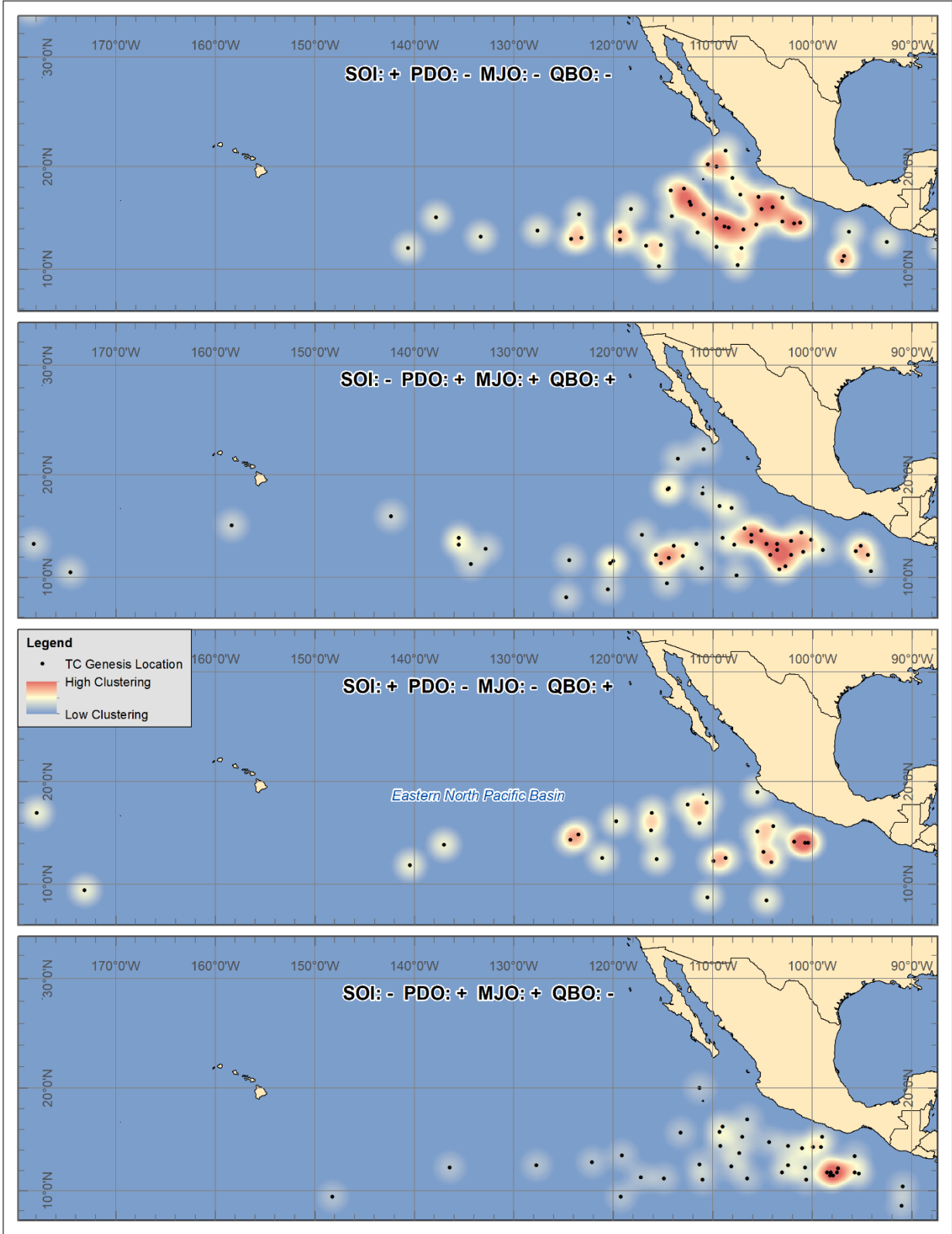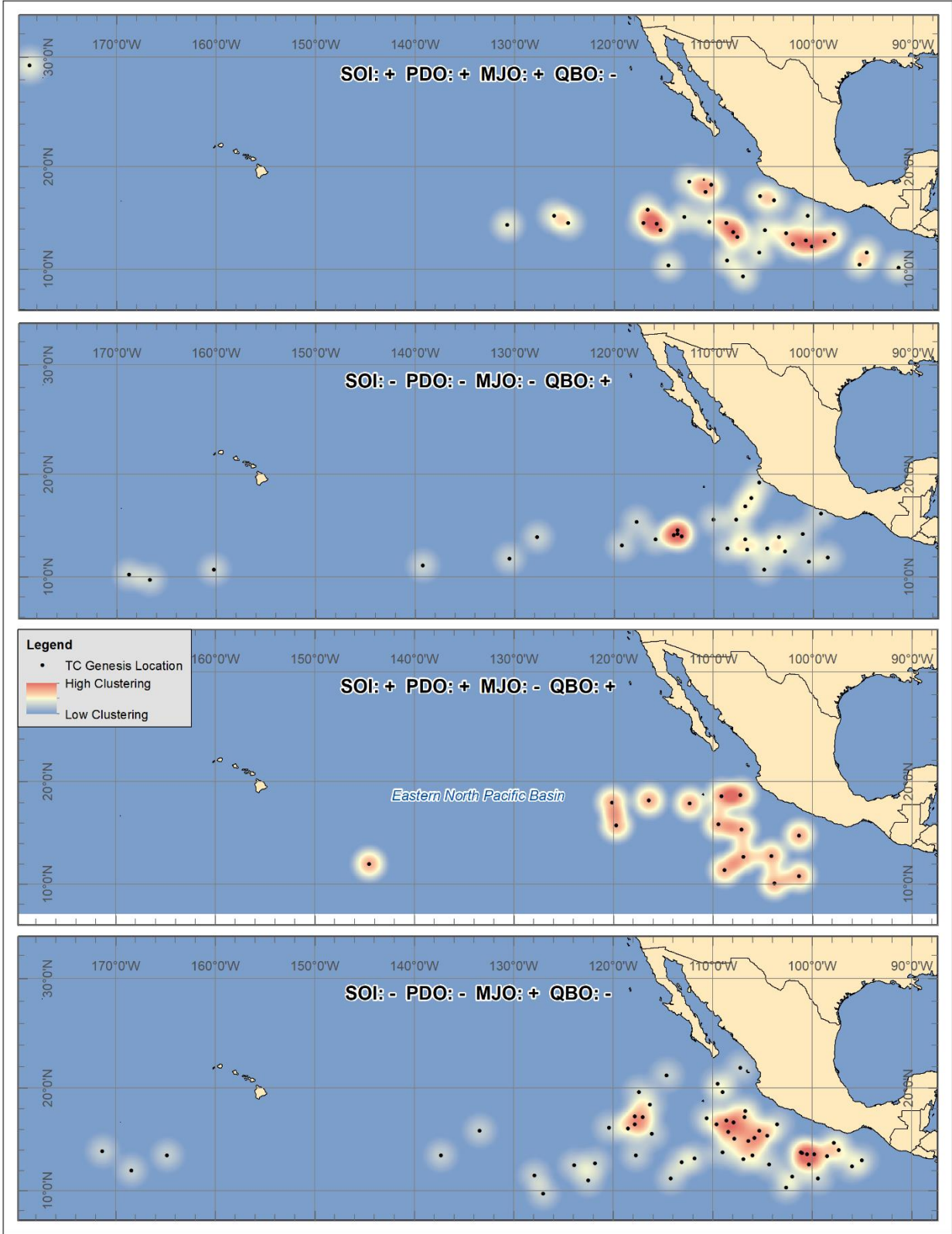**WGS84:** World Geodetic System 1984

WP: West Pacific (teleconnection)

APPENDIX C:
EASTERN NORTH PACIFIC BASIN COMBINATION MAPS